HEAT SHIELD CONCEPTS AND MATERIALS FOR REENTRY VEHICLES

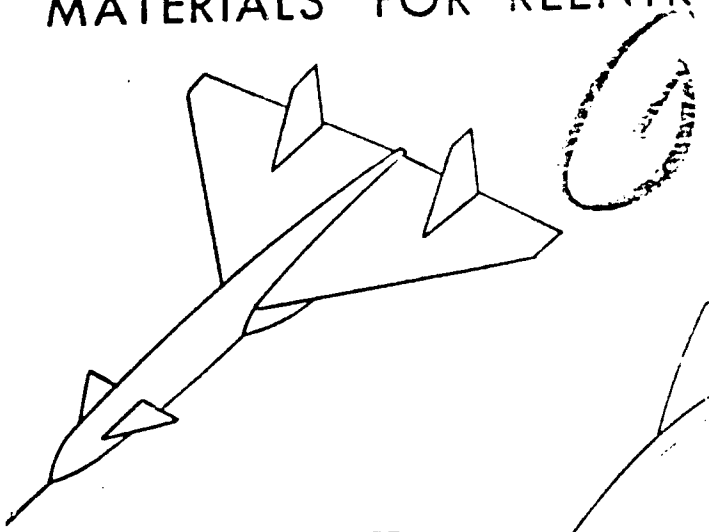

SUPERSONIC AIRCRAFT

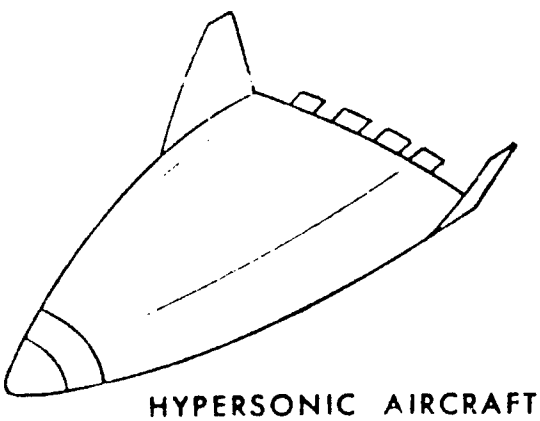

HYPERSONIC AIRCRAFT

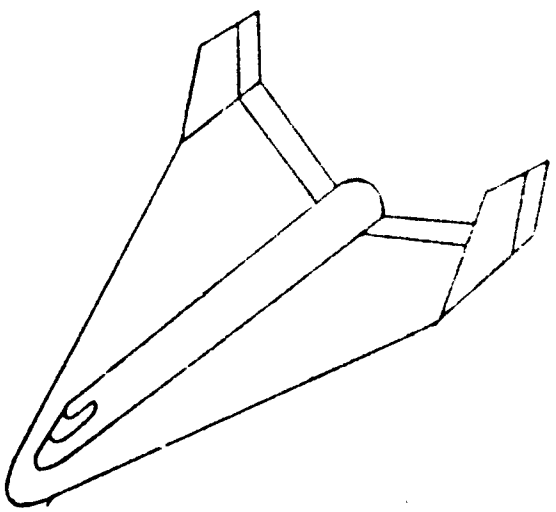

HIGH L/D REENTRY VEHICLE

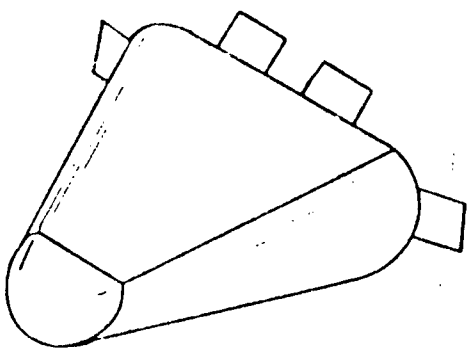

LOW L/D REENTRY M-1 CONFIGURATION

JULY 15, 1963

EDITED BY: W. NIEHAUS

"EXHIBIT"

Accompanying the presentation on Heat Shield Materials will be an exhibit showing applications of the Aeronca Thermantic "Astroshield" concept. It is believed that the working model made for the Air Force by Aeronca on AF 33(657)-7151 (Work Statement No. 12) would be most appropriate for this purpose. As stated in this work statement, the model display is constructed to show the typical system configuration and includes component detail such as "Astroshield" panel construction, joint design, insulation, support structure design and mission capabilities.

1. INTRODUCTION

The present research at Aeronca under contract with the Manufacturing-Technology Laboratory and the Flight Dynamics Laboratory branches of the U. S. Air Force, WPAFB, in the field of thermal protection systems for reentry vehicles is the natural result of its evolution from one of the nation's first light plane manufacturers in 1928 to its present status as one of the nation's most active fabricators of honeycomb type structures.

Presently, Aeronca has three major locations at which space type work, research and related activities are being performed. The three locations and the general type of space work associated with each are:

1. Middletown Division: Antenna Systems, Aircraft Components, Missiles Space Heat Shield Research, Honeycomb structures
2. Aerospace Division (Baltimore): Optimal Control Theory and Associated Electronic Gear, Electronics for control, data handling and detection; Communication Electronics Systems Design
3. Aerocal Division(California): High temperature structures, Airframes for weapon systems and transports, ejection devices, missile packaging, ordnance devices, practice weapons

The purpose of this paper is to discuss thermal protection systems and the Thermantic Structure developed by Aeronca Manufacturing Corporation, and funded by the Air Force, at its' Middletown Division. Aeronca has in recent years been engaged in the development of materials and structures to withstand temperatures in excess of 3000°F for extended periods of time(approximately one hour) and to resist

severe noise and dynamic loads associated with space vehicle flight. Aeronca's basic approach to the composite heat shield concept has been to utilize a reinforced ceramic heat shield to protect the vehicle from its heating environment. The heat shield, made of a low density ceramic foam reinforced with a honeycomb cell structure, is capable of maintaining an internal temperature suitable for the survival of both man and sensitive equipment. The thermantic structure uses a conventional load bearing panel fabricated from alloy sheets brazed to stainless steel honeycomb and this panel brazed to the ceramic honeycomb reinforcement. This "Astroshield" concept offers the combined advantages of high temperature resistance, lightweight, thermal shock resistance, chemical stability and high strength. In the course of this development program, several lightweight ceramic compositions have been fabricated in porous forms with satisfactory mechanical and thermal properties for re-entry vehicle structures. The most promising have been silica (S.G. .5 and 3000°F M.P.), alumina (S.G. .5 and 3400°F M.P.) and zirconia (S.G. 1.1 and 4200° F M.P.) These ceramics when reinforced with superalloy or refractory metal honeycombs form durable insulating heat shields which radiate almost all heat input back into space. High emissivity ceramic coatings reduce radiant heat transmission through the structure to approximately 2% during re-entry flight.

The Aeronca Thermantic "Astroshield" concept is oriented towards several applications involving space vehicles. The radiation cooled structure can be used for almost the entire external surface of lifting body shaped vehicles, nose caps, leading edges, portions of fuselages and winged sections of aerospace vehicles. In addition, the research in lightweight porous ceramics

has produced materials which are also useful in other related fields where high heat or energy environments exist. Examples are a porous beryllium oxide composition for nuclear application as a heat insulator and neutron reflector, a zirconia based insulation to protect the nose spike of a training missile produced by Aeronca, and a composite thermal protection system for use in reducing the base heating problem associated with boost and launch vehicles.

The following discussion presents the concept of the Aeronca "Astroshield" in detail, its composition and capabilities. In order to better understand and appreciate its potential, a brief description of the general classes of heat shields along with typical reentry environments is given. Also briefly described are the types of reentry vehicles to which these heat shield concepts have or will be applied, how the 'Astroshield" compares with these other heat shields, and specific areas where the Aeronca concept may be applicable.

II. Hypersonic Flow Regimes

It is convenient for hypersonic flight[1] to define the flow regimes in terms of the molecular phenomena encountered during the development of the flow field as a space vehicle enters a planetary atmosphere (Fig. 1). This figure shows a relatively simple classification scheme, as well as two typical trajectories for suborbital entry into the earth's atmosphere.

At the highest altitudes, the mean free path is large compared with a typical vehicle dimension, such as nose radius. Because of the extreme rarefaction

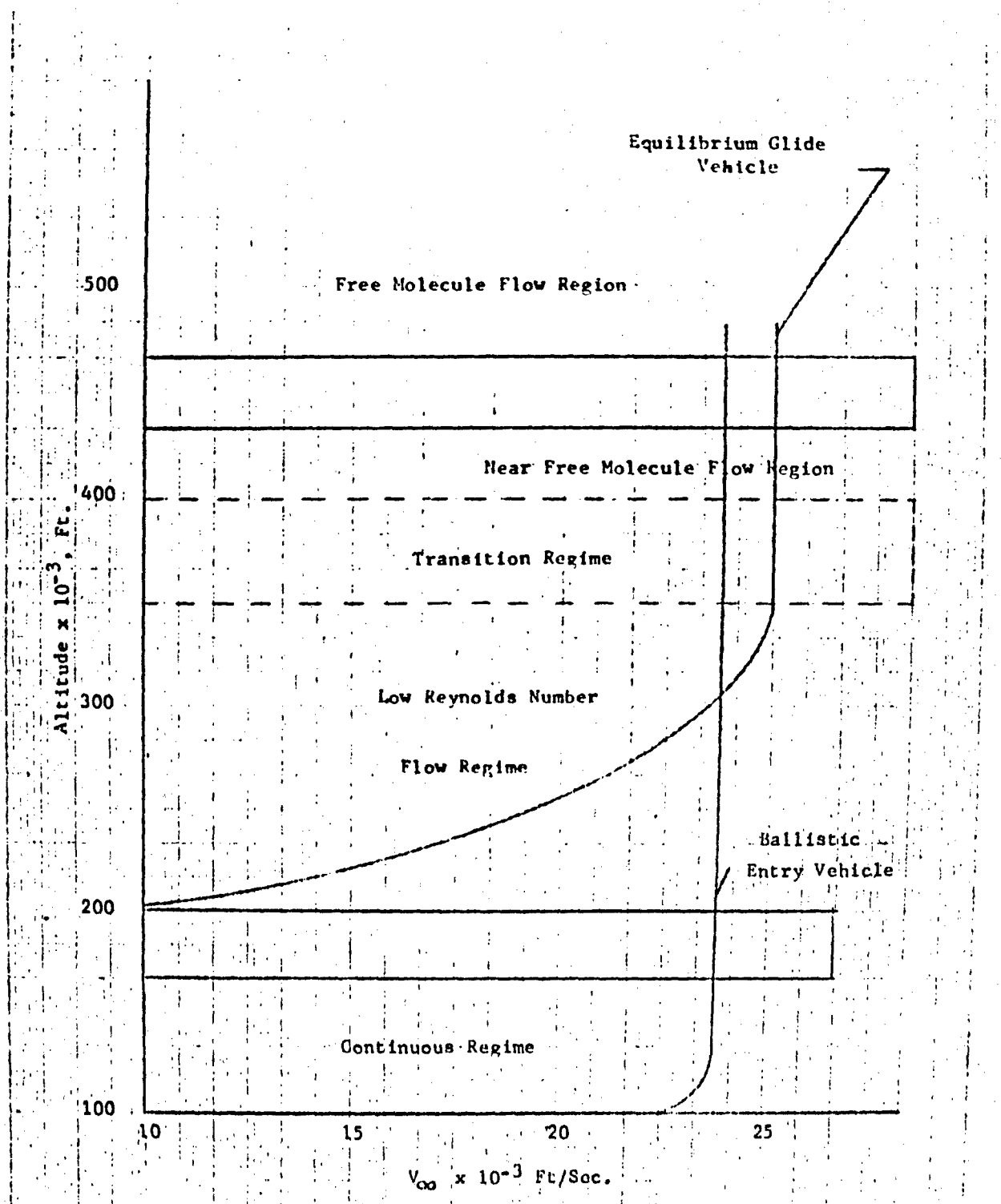

Figure 1 High Altitude Hypersonic Flight Regimes (Ref. 1)

of the gas, the reflected gas molecules collide infrequently with the incident particles, and all interactions involving energy transfer therefore tend to occur immediately at the vehicle surface. This is known as the free molecule flow regime.

As the vehicle penetrates the stratified atmosphere more deeply, the density of the ambient gas increases, and the frequency of collisions between incident and reflected molecules increases to such an extent that the velocity of the incident stream is perturbed by the presence of the molecules issuing from the vehicle surface. This is known as the near-free molecule flow regime.

As the free-stream density continues to increase, the extent of the interaction between incident and reflected molecules is more pronounced and the zone of interaction begins to coalesce into a shock wave. This is known as the transition regime, since it delineates the onset of the region in which macroscopic gas phenomena start to dominate over microscopic phenomena in the bulk gas flow.

At still lower altitudes, a fully developed shock wave is present in the flow a finite distance upstream of the vehicle, and the flow between the shock wave and the vehicle surface is fully viscous. In this low Reynolds number flow regime, one can distinguish further between conditions of partial or full merging of the structure of the shock wave with that of the viscous layer at the vehicle surface.

At the lowest altitudes, the shock Reynolds number, which is directly proportional to the free-stream density, is sufficiently large so that the

viscous layer separates into two distince regions in the flow field. The shock-wave thickness decreases and behaves essentially like a discontinuity in the flow. The viscous layer thickness decreases and becomes a thin boundary layer.

It is noted that the bands shown in Fig. 1 represent the approximate extent of the smooth transitions from one flow regime into the adjacent regime where, for the sake of illustration, the nose radius of the vehicle was assumed approximately equal to 0.1 ft.[1] An increase in vehicle nose radius has the effect of shifting all of these regimes to a higher altitude; conversely, a very small object will find itself in a rarefied flow environment down to relatively low altitudes.

III. Reaction of Air to Hypersonic Flow

The temperature immediately downstream of the shockwave increases as the square of the Mach number ahead of the shock wave. At the Mach number of approximately twelve, the temperature is about 10,000°F., the temperature at the surface of the sun. At a Mach number of 20, the temperature is over 30,000°F. The region of extreme temperatures is extensive at the nose but farther back on the body is confined to a thin layer.

Air at these high temperatures exhibits some properties which must be taken into account in any theory which would predict temperatures at the surface of the vehicle. According to the kinetic theory of gases, the temperature of any gas is proportional to the mean kinetic energy of the random translational motion of the particles that make up the gas. If a certain amount of energy is added to a gas (by adding heat and/or by doing work on the gas), and if all

of this energy goes into the translational motion of the particles, a certain temperature rise will occur. At higher energy levels, however, the gas particles can absorb energy in other ways. In addition to translational motion, there are other degrees of freedom - rotational and vibrational - and there are the processes of electron excitation, dissociation, and ionization. Dissociation is the process in which the atoms of the molecule become sufficiently excited to overcome the binding force in the molecule and become separate particles. Ionization occurs when electrons within the atom gain sufficient energy to break free.

There are several important points about these processes:

1. For a given gas, there is a definite energy level associated with the attainment of equilibrium in each of these states.

2. If heat is added or work done on the gas, the increase in translational motion of the particles will produce a temperature rise. If energy is absorbed by other processes such as an increase in rotational or vibrational motion, or by an increase in electron excitation, or by the dissociation or ionization, the temperature rise will be reduced. We may therefore refer to this as a "heat sink" effect. The implication is, of course, that we are now dealing with a gas which does not have a constant specific heat. With respect to the aerodynamic heating problem, it is important to note that while the "heat sink" effect lowers temperatures, this energy will be given up when re-combination takes place and surface temperatures will go up.

3. Finally, there is a finite time required for each degree of freedom to reach a state of equilibrium. This is known as the "relaxation time".

It is an important factor because, if the flow velocity is known the relaxation time can be transformed into a relaxation distance, and this can be related to the physical distances between the shock wave and the body.

The relationship between "relaxation time" and the time for a particle to travel from the shock wave to the body is shown on this Fig. 2.(2) The velocity of the vehicles of interest is plotted versus the ratio of the dissociation time to the flow time. The dissociation time is the relaxation time, which has been defined, while the flow time is the time it takes a molecule to travel from the shock wave across the shock layer to the body surface.

Three flow regimes are shown. If purely molecular excitation pertains, the flow is said to be frozen. The time for dissociation is large relative to the time for a particle to travel from the shock wave to the body. The leading edge radius of the wing of a hypersonic glide vehicle is relatively small - consequently the shock wave is a short physical distance ahead of the leading edge - so the flow is frozen at the leading edge. Points farther aft on the wing lie on the region of non-equilibrium, that is, there is time for some dissociation to occur, but equilibrium conditions are not attained. Other vehicles having larger leading edge radii, such as satellites, as well as the nose of the body of the glide vehicle, would have flows in the region of non-equilibrium. The blunt, ballistic nose cone with a strong shock wave well forward of the nose would be characterized by equilibrium flow. Shown also on Fig. 2 are the approximate velocities where maximum heating occurs. The satellites and escape vehicles go through maximum heating at higher velocities than do the other types shown.

FIGURE 2- DOMAIN OF FROZEN FLOW AND DISSOCIATION EQUILIBRIUM (2)

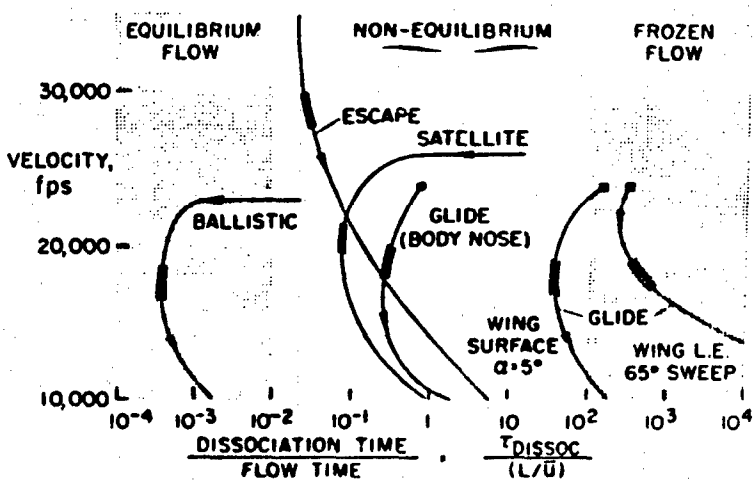

IV. Reentry Environment

Fig. 3 shows the maximum stagnation heating rate plotted as a function of total heat load and equilibrium temperature for a band of combination's of the current concept of normal re-entry vehicles.[3] The upper edge of the band corresponds to re-entry of a nonlifting vehicle which experiences a maximum deceleration of about 8g. The lower edge of the band corresponds to a vehicle having an average lift-to-drag ratio during reentry of about 2.5. The associated times of reentry increase from about 4 minutes at the upper edge of the band to about 70 minutes at the lower edge of the band.

The location within the band is associated with wing or area loading and with entry attitude and velocity. Very lightly loaded vehicles fall in the lower end of the band, while vehicles 'having greater weight per unit area are shifted upward along constant time lines. The most severe heating conditions are encountered by vehicles which combine high wing loading with high lift-to-drag ratio. On a particular vehicle, a considerable range of heating conditions will be encountered from the stagnation point to the rearward areas as we shall see a little later in the discussion. When variations in lift-to-drag ratio, wing loading and vehicle configuration are considered, it is apparent that thermal protection systems must be provided which can handle heat loads varying from about 1,000 Btu/ft^2 to over 100,000 Btu/ft^2, and which can survive heating rates of less than 10 Btu/ft^2 sec to over 100 Btu/ft^2 sec. Radiation equilibrium temperatures associated with these heating rates are shown on the scale at the right. As noted, they are computed with the assumption that a material emissivity of 0.8 is achieved.

Figure 4 indicates the flight corridors in terms of altitude and velocity.[4] The shaded area indicates the region that can be explored by the X-15 research

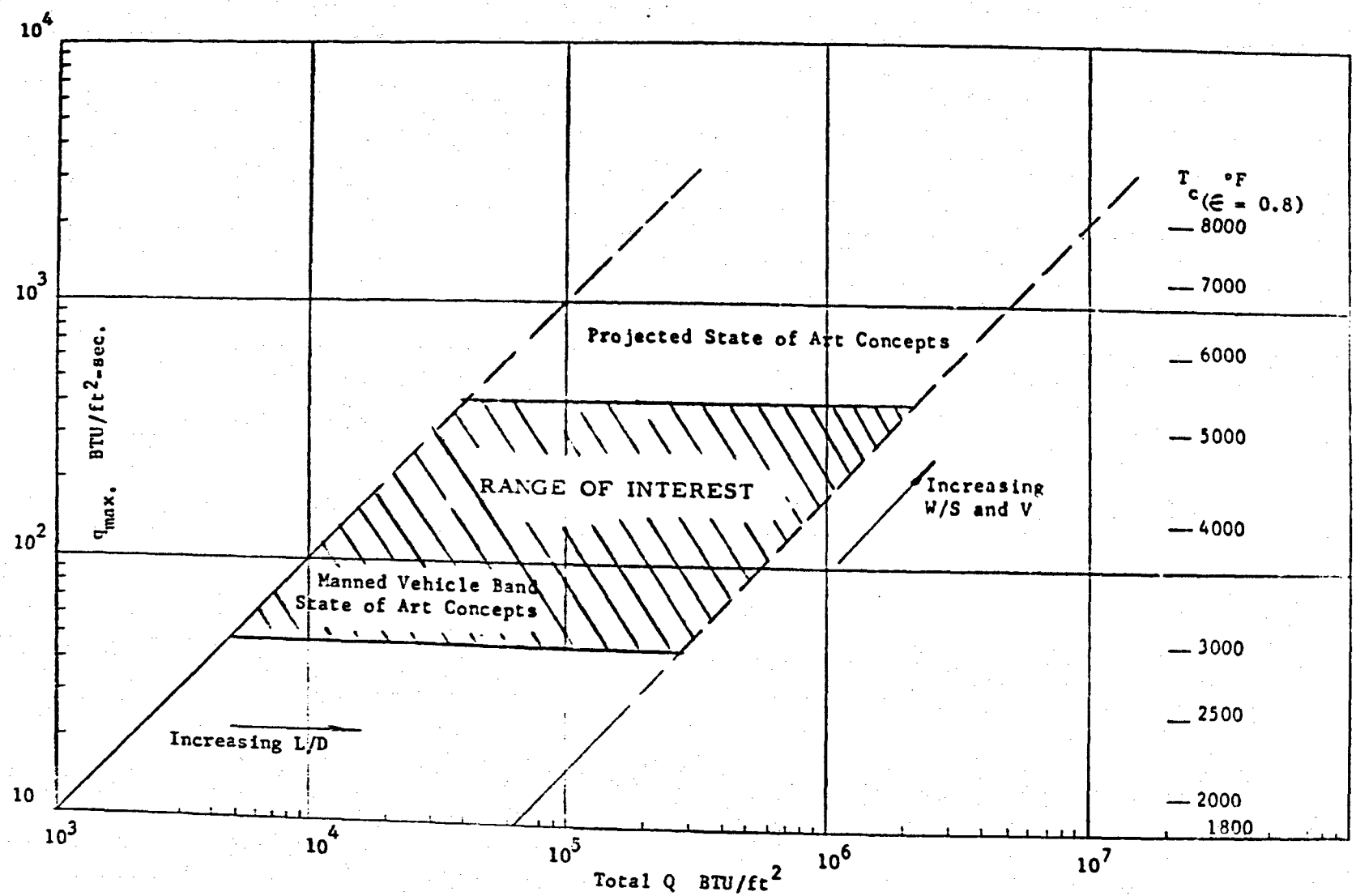

Figure 3. Re-Entry Vehicle Band (3)

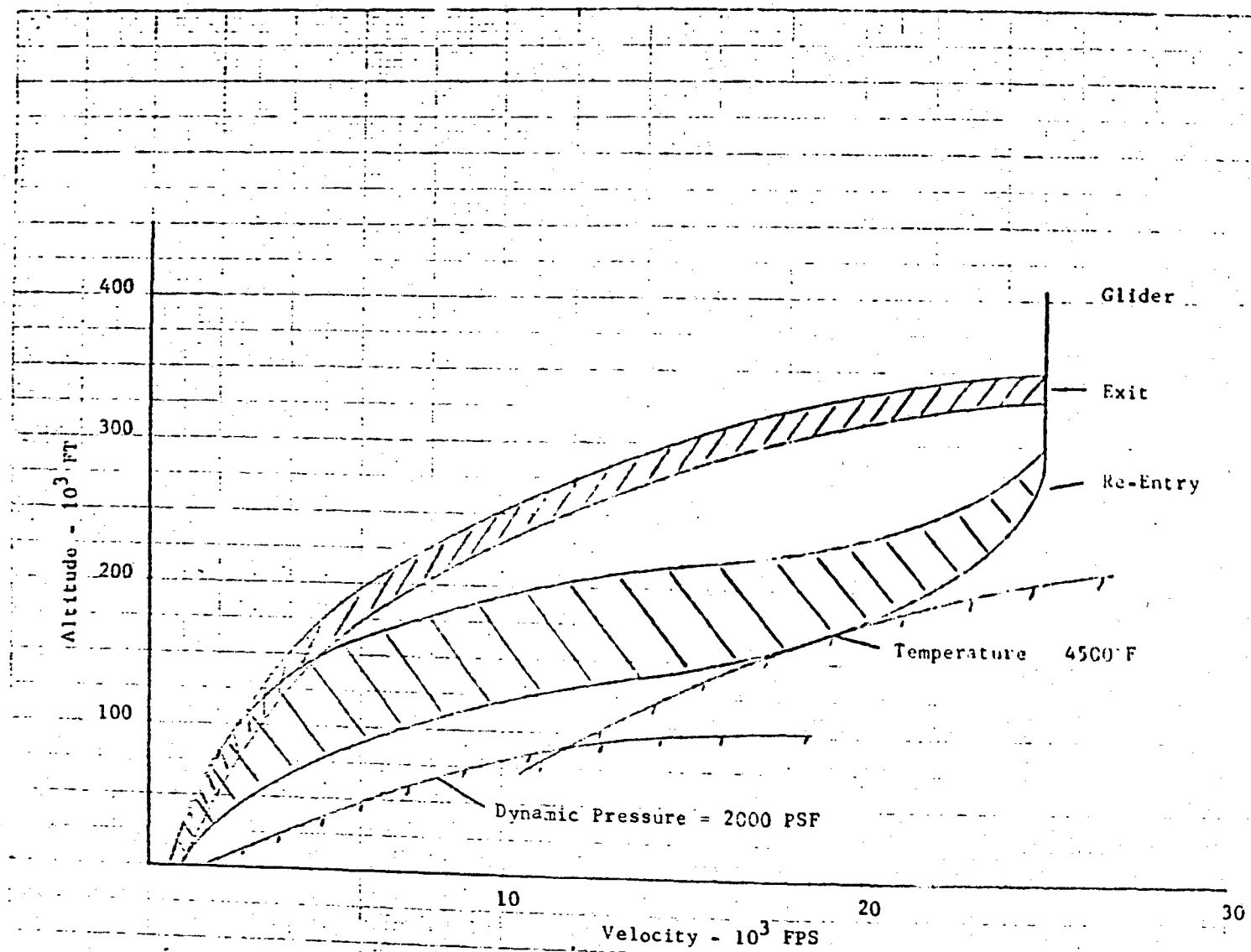

Figure 4 Typical Flight Corridors for Winged Aerospace Vehicles (4)

airplane. The glider is launched along an exit trajectory as shown and returns within the indicated reentry corridon. The lower limits of the reentry corridor are defined partly by temperature and dynamic pressure. The 4000° F temperature line defines a radiation equilibrium temperature for a 1-foot-diameter nose with an emissivity of 0.8. Note that the reentry glider does not experience severe heating during exit because the exit corridor does not appear close to the indicated temperature line. Note that the exit corridor is near the curve for 2,000 pounds per square foot dynamic pressure. The highest structural temperatures occur at the point of tangency between the flight corridor and the temperature curve.

No specific flight corridor is indicated for the hypersonic airplane. If the vehicle possesses orbital capability, reentry with a hypersonic airplane would be made in approximately the same corridor as that for the glider.

V. Classes of Reentry Vehicles

Figure 5 provides a brief look at classes of vehicles and re-entry corridors for which aerothermoelastic problems are of practical concern.[5] The shaded portions show possible operating regions of altitude and speed; also shown are dynamic pressure contours q and nominal radiation equilibrium temperature contours. Scanning the figure, we see essentially lunar re-entry speeds on the far right (Apollo); then earth orbital speeds; indication of ballistic steep re-entry; winged vehicle re-entry -- e.g., the X-20 (Dyna-Soar) -- and antimissile range covering extreme ranges of dynamic pressure a factor of the utmost significance for aeroelastic problems; the X-15 research airplane; and supersonic airplanes. The small dark area indicated in the transonic region represents a potentially troublesome design area for all these vehicles.

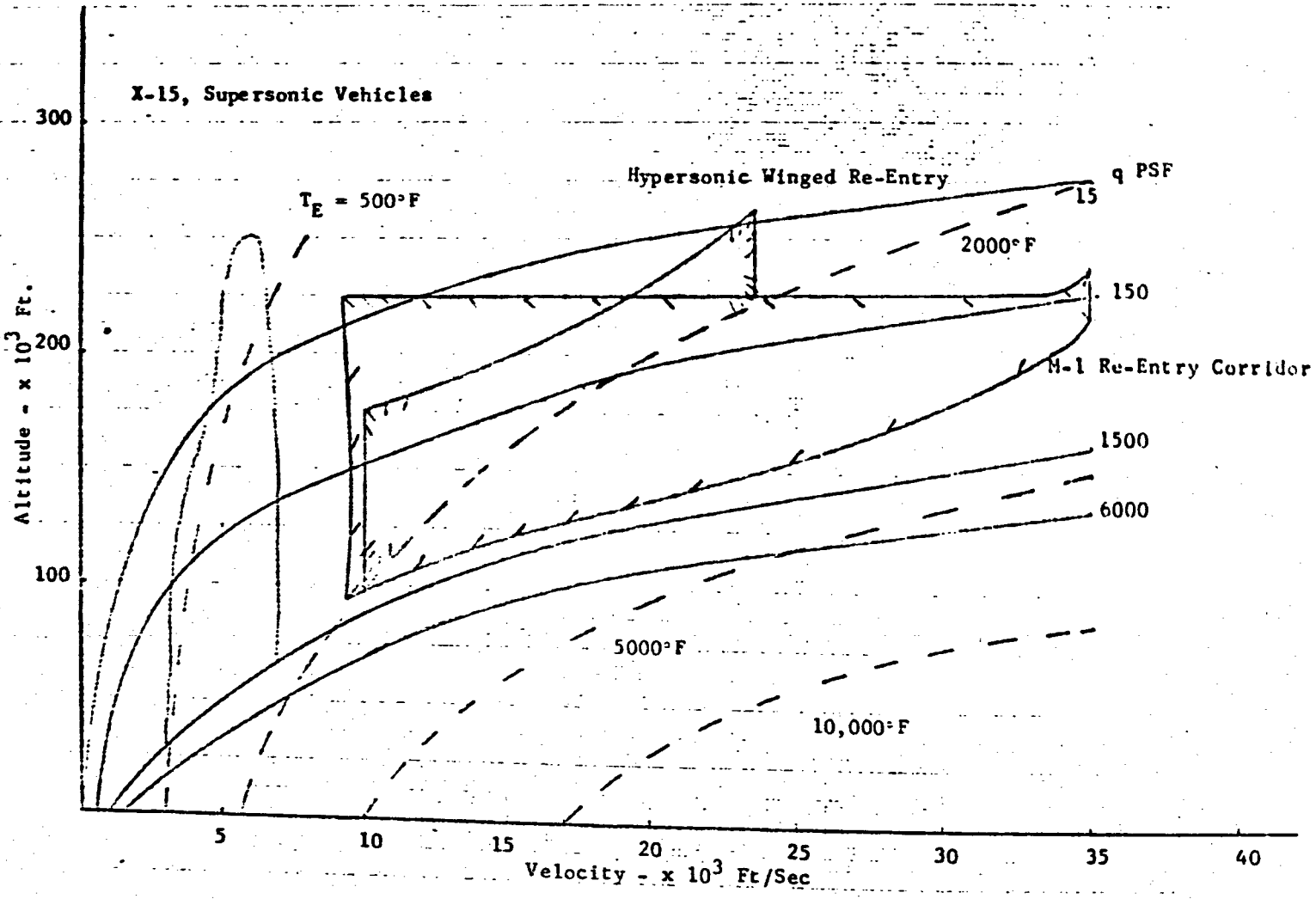

Figure 5 Flight Corridors of Various Vehicles Indicating Nominal Dynamic Pressures & Temperatures (Ref. 5)

Fig (6) provides a more specific flight trajectory for several re-entry type vehicles.[6] Notice that the higher velocity vehicles reach their points of maximum heating at a higher altitude and higher velocity than the orbital and sub-orbital vehicles.

Aerospace vehicle concepts and their respective missions are by no means exhaustive.[7] The aerospace vehicle classes shown in Fig. 7 will be defined for the purposes of the present discussion.

Fig 7a shows a supersonic aircraft concept -- Aircraft in this category are winged with relatively high L/D (approximately 7.0); and have conventional monocoque or semimonocoque structure. Cruise speeds lie in the Mach number region from 2.0 to 4.0 with altitudes ranging up to approximately 100,000 ft. Structures will be subjected to steady state temperatures in the vicinity of 600° to 800°F during cruising flight; and the design dynamic pressure may be as high as 2,000 psf depending on the mission altitude. Examples of this class are: (a) supersonic transport, (b) supersonic bombers (High and low altitude), and (c) early version of the recoverable booster system.

Fig 7b shows a hypersonic aircraft -- These aircraft are winged with moderable L/D (approximately 4.0). By virtue of the extremely low fuel density, they will require high volume and a heat protected or insulated structure. Maximum speeds will be in the vicinity of Mach 12.0 at altitudes up to 250,000 ft. At these conditions, however, the flight time will be relatively short. Maximum steady state and transient temperatures of approximately

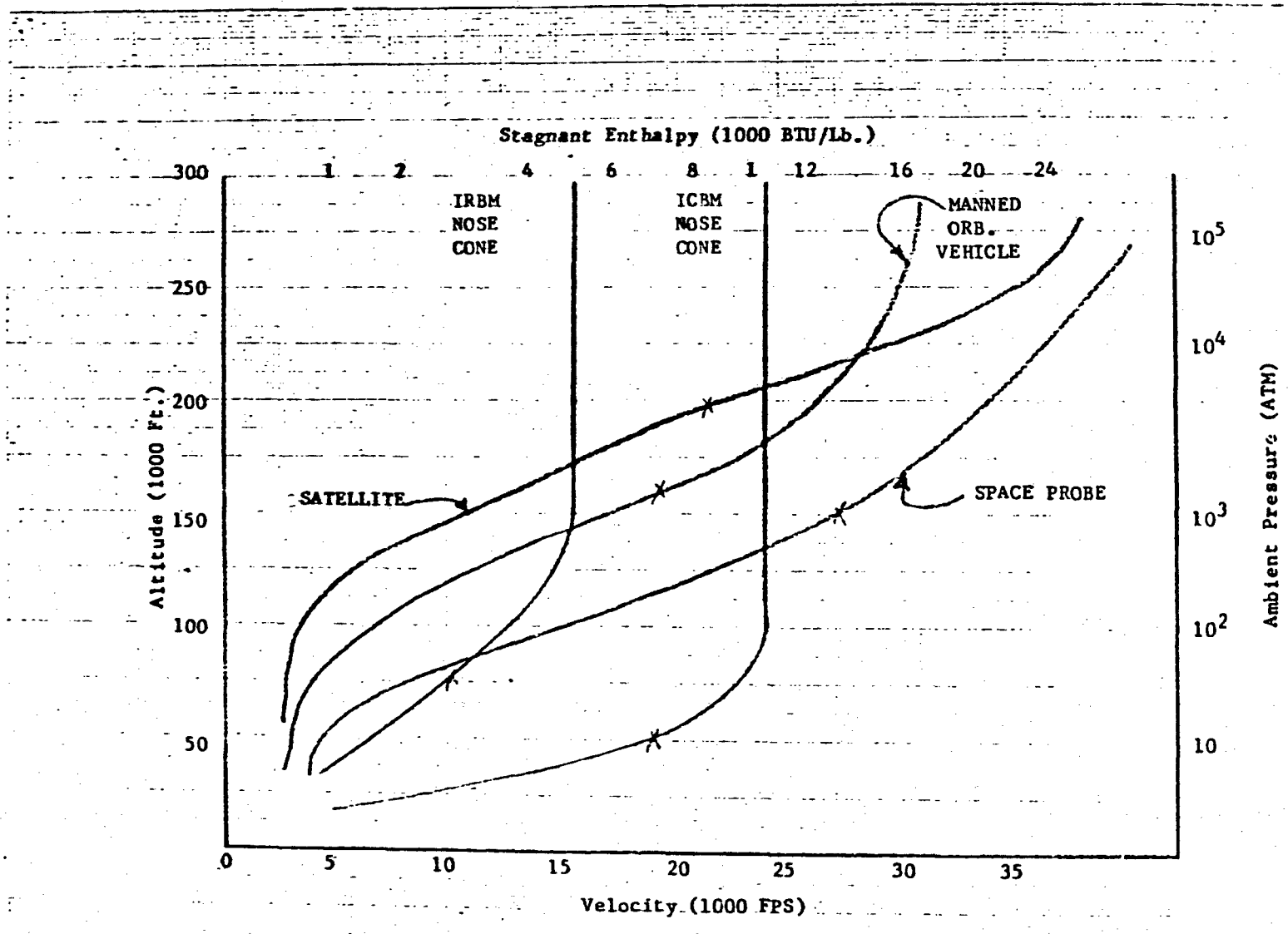

Figure 6 Flight Trajectories & Approximate Peak Heating Points (X) (Ref. 6)

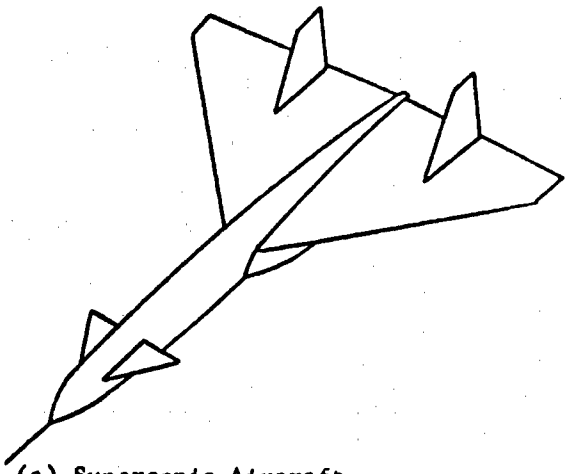

(a) Supersonic Aircraft

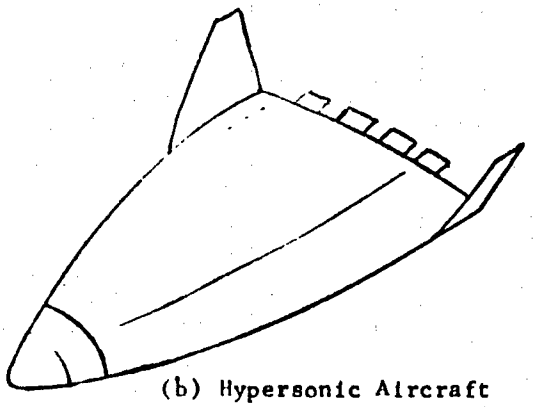

(b) Hypersonic Aircraft

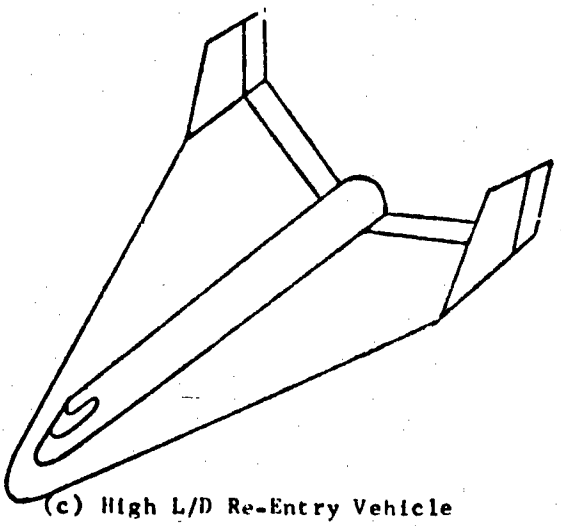

(c) High L/D Re-Entry Vehicle

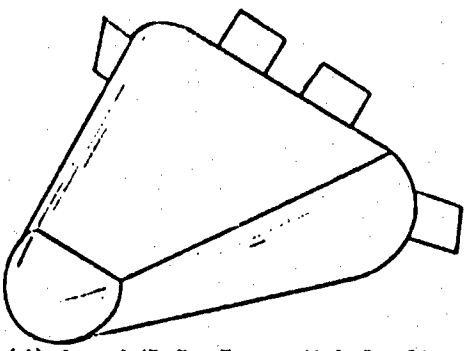

(d) Low L/D Re-Entry M-1 Configuration

Figure 7 Aerospace Vehicle Concepts (7)

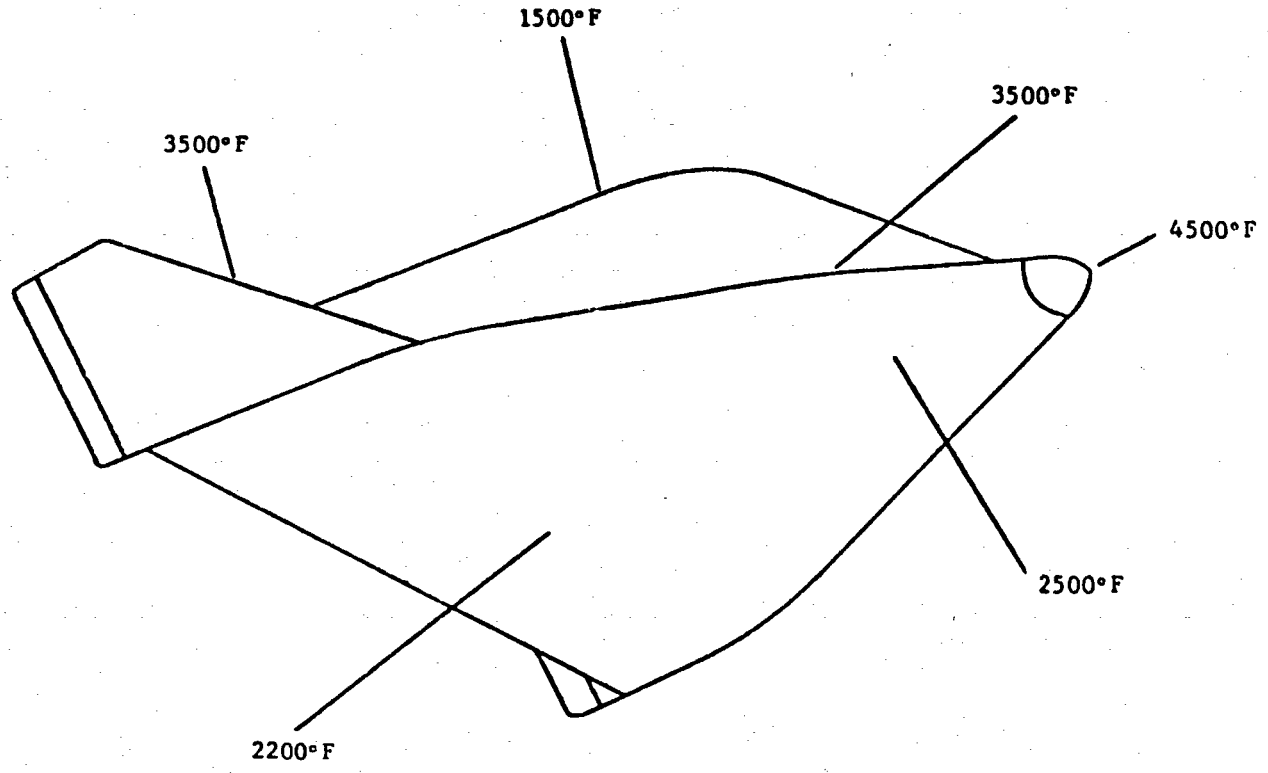

Figure 8 Typical Surface Radiation Equilibrium Temperatures for A Re-Entry Glider (4)

1500° to 2000° F may be expected although the dynamic pressures at the high temperature design point will be less than 1000 psf. At lower altitudes and temperatures, the dynamic pressure limit will be approximately 2500 psf. Typical examples of this type of vehicle are (a) advanced recoverable booster and (b) hypersonic bomber.

Fig 7c shows a high L/D re-entry spacecraft -- These vehicles have relatively low wing loadings with an L/D in the vicinity of 2.0. Variable aerodynamic geometry, and external drag devices may serve, in conjunction with reaction and aerodynamic controls, as a primary means of re-entry flight path correction. The structure may be of the heat protected truss type, forced cooling, or hot refractory metal configuration. For satellite velocity re-entries, a maneuvering, maximum heating load (as opposed to a maximum heating rate) trajectory will be flown with maximum temperatures near 4500°F in local regions such as leading edges, nose, etc. Design dynamic pressures will be of the order of 1000 to 1500 psf. Boost-glide vehicles are typical of this class. Fig (8)

Fig 7d shows a low L/D re-entry spacecraft -- Vehicles of this type have no wings but nevertheless achieve a limited lifting capacity (L/D 0.5) from the basic body shape. The structure is heat protected either by means of heat sinks or ablative materials. Either reaction controls or combined aerodynamic-reaction controls (flaps) are used to provide limited maneuverability. The re-entry trajectory is determined primarily by re-entry conditions and the ballistic coefficient ($W/S\ C_D$). These vehicles will be utilized primarily

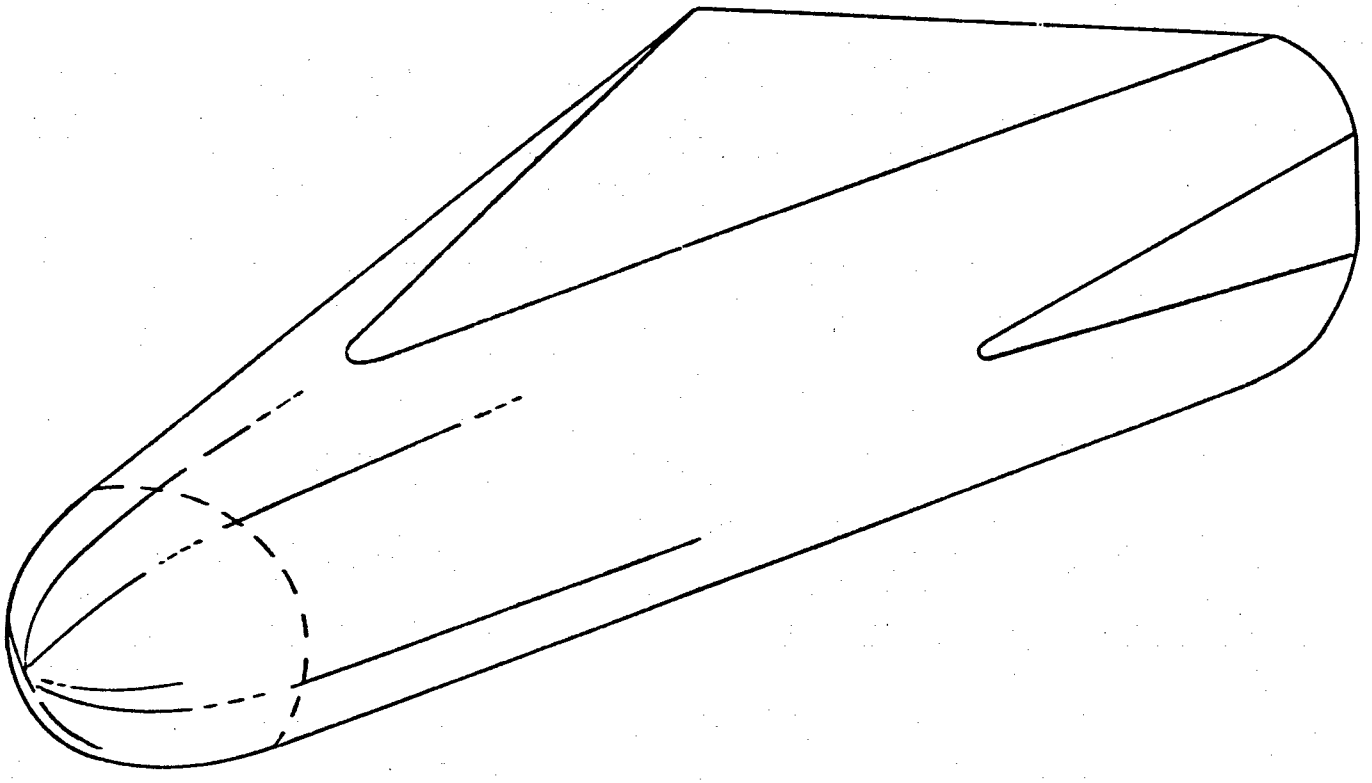

Figure 9 Re-Entry Lifting Body (8)

for "deep space" or "long time" missions where the relative inefficiency of the re-entry is offset by the volumetric efficiency of the unwinged aerodynamic shape. Re-entry trajectories will result in high heating rates and critical temperatures of the order of 5000°F with dynamic pressures of approximately 2000 psf. Current examples of this type of spacecraft are: (a) Mercury, (b) Apollo, and the vehicle shown in Fig (9).

VI. Absorptive Heat Protection Systems

The principle of absorptive systems is the absorption of the generated heat by a permanent or expendable heat sink. An example of the former is a metallic shield of high heat capacity and low density, such as beryllium, while examples of the latter are the many currently available ablating materials possessing high heats of ablation such as phenolic-asbestos and Teflon. (9)

Absorptive Systems are especially suited for applications where high heating rates are experienced, since in these systems temperature is not particularly related to heating rates. On the other hand, the weight of the system may become prohibitive for the large total heat inputs that are usually associated with long heating periods. A sufficient amount of sink material must be carried by the vehicle to absorb most of the heat generated during the entire mission.

VII. Heat Sink System

The simplest system of cooling during thermal flight operation is the heat capacitance or permanent heat sink system. By this method, a sufficient mass of material is provided to absorb the heat being generated by the re-entry vehicle. Sufficient mass must be provided to limit the temperature rise to a workable level. In order to be a good solid phase heat sink candidate, a material must have a high melting point, high heat capacity, high density

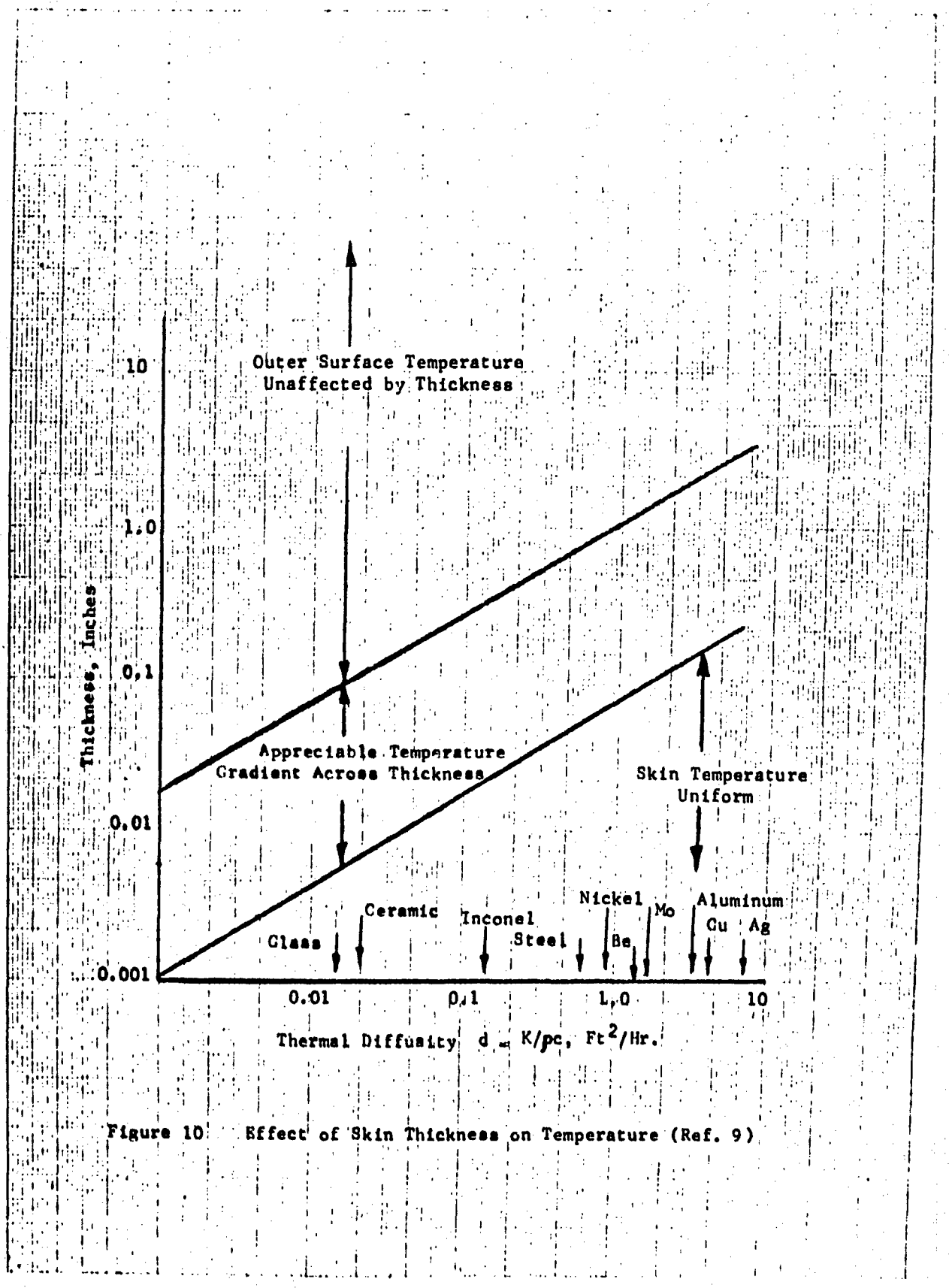

Figure 10 Effect of Skin Thickness on Temperature (Ref. 9)

Material	Melt. Temp. °F	Average * Conductivity BTU/Hr-Ft-°F	Average * Spec. Heat BTU/Lb-°F	Average Density Lb/Ft^3
Graphite	6600 (sublimes)	40 (90 - 18)	0.42 (0.20 - 0.47)	105
Titanium Carbide	5880	4.5 (16 - 3)	0.205 (0.12 - 0.22)	306
Boron Nitride	5432	7 (10 - 6)	0.22 (0.11 - 0.25)	138
Titanium Nitride	5342	6 (26 - 4)	0.21 (0.14 - 0.24)	339
Magnesium Oxide	5072	6 (17 - 4)	0.31 (0.22 - 0.34)	216
Silicon Carbide	4892 (decomposes)	30 (70 - 8)	0.30 (0.16 - 0.40)	198
Beryllium Oxide	4620	25 (130 - 8)	0.43 (0.20 - 0.50)	172

* Nos. in parentheses represent approximate range of properties from room temperature to melting temperature

Figure 11 Properties of Heat Sink Materials (10)

and heat capacity product (if volume is a consideration) and high thermal conductivity so that the surface temperature does not exceed melting. The efficiency and success of this system depends on the thermal diffusivity $k/\rho c$ of the heat sink material. Fig. 10 illustrates some limitations of such a system. It is noted that for materials with low thermal diffusivity the main addition process soon reaches the point of diminishing returns. For such materials, such as ceramics, increases in mass soon reach a point at which further increased thickness will have little effect on the temperature of the heated surface. Even highly conductive materials, such as aluminum, copper, or silver approach this point in thickness of about an inch or so.

Cooling by this system is limited total heat loads on the order of 10^4 BTU/ft^2, which is characteristic of ballistic re-entry type vehicles. The reason for this limitation is that after a given flight time melting begins at the surface and is independent of the thickness. In other words, the thermal diffusivity is such that heat cannot be soaked or absorbed fast enough by the inner layers to prevent the outer layer from melting. Properties of several heat sink materials are given in Fig 11.

VIII. Ablative Systems

It is obvious from Fig. 10 that capacitance cooling, although simple, is an inefficient means of coping with extremely high heat fluxes associated with certain reentries or with sustained period of thermal flight. Consequently, other means of cooling for operating beyond these limitations must be used. One such method is ablative or expendable heat sink cooling. This method offers many advantages and is applicable over a wide variety of heat fluxes. Similarly, it can be made to operate at a relatively low surface temperature.

This capability has an important side effect in that it can reduce the internal cooling problem, if internal equipment is involved.

The ablative process is illustrated in Fig 12.(9) In this process the material will first act as a heat sink. As a critical temperature is reached, a thin layer of material at the surface will begin successively to melt, vaporize, depolymerize, or decompose chemically. The coating materials chosen for this application are such that as this transformation takes place at the surface large quantities of heat are absorbed. That is to say, the material has a large heat of fusion, etc. The quantity of heat required to bring about this change of state will depend on the characteristics of both the ablating material and the surrounding atmosphere produced.

Moreover, as the material is vaporized, the gases or products of decomposition enter into the boundary layer, and being much cooler than the boundary-layer air, they form a thin but effective film that greatly reduces the heat transfer to the surface.

In Fig. 12 ablation is taking place at the surface and gases are being produced. For any given flow, the gas so produced diffuses through the boundary layer and as a mixture with the air is carried off by convection. This action is due to the pressure gradient in the boundary layer and to the shearing force due to the presence of the body wall.

In the selection of a suitable material for heat protection by the ablative process, the thermal conductivity of the material should be as low as possible, so as to confine the high-temperature zone at the surface (Fig. 12), to the thinnest

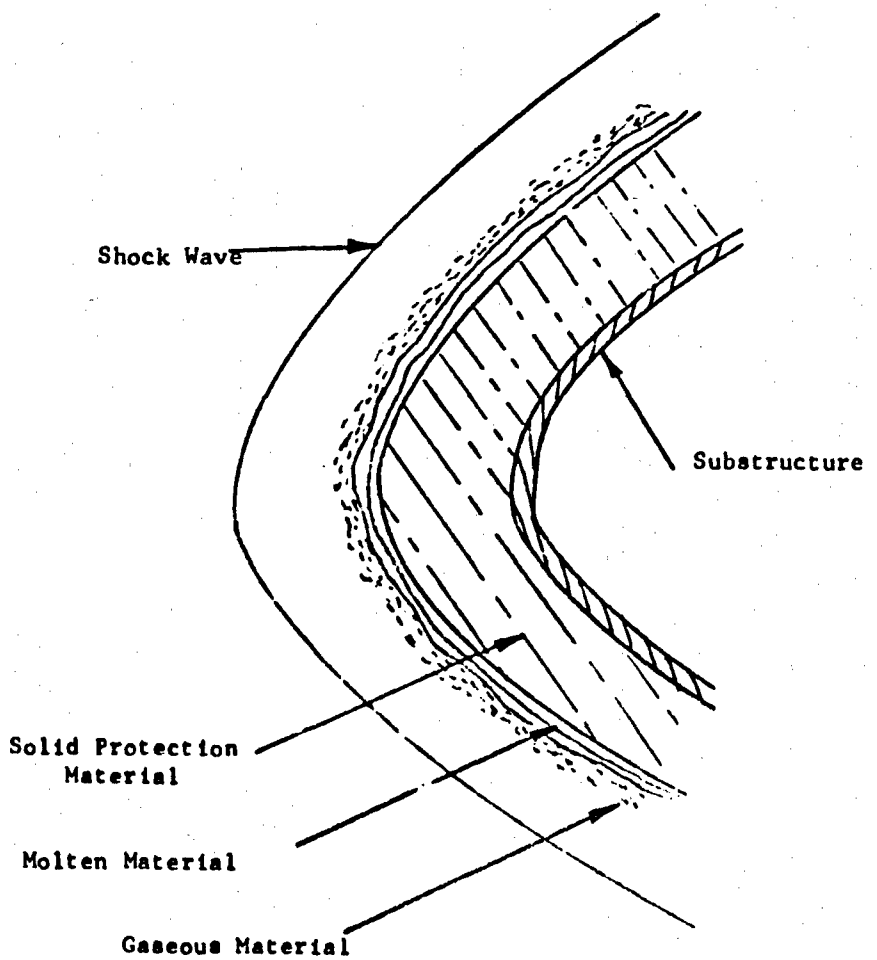

Figure 12 Ablative Process in Stagnation Region (Ref. 9)

layer possible. Likewise, in order to reduce the rate of mass loss, and hence the surface, the viscosity of the material should be high so that it is not carried away by the shearing action of the boundary layer.

The products of decomposition should preferably have a high Prandtl number. (9) Since it is desirable to have the effective mean specific heat of this gas-air mixture in the boundary layer as large as possible, it naturally will be largest when the specific heat of the gas produced in decomposition is large compared to that of the air in the boundary layer.

Schmidt and Prandtl numbers will be the governing parameters, controlling the thermal shielding effects of the generated gas. For maximum shielding, when the specific heat of the gas is smaller than the boundary-layer air, the Schmidt number of the gas should be large. Likewise, the Prandtl number should be large. When the gas has a higher specific heat than the boundary-layer air, the Prandtl number should be large, but the Schmidt number small.(9)

The success of the ablation shield results first from the fact that it is not heating-rate limited, and second from its ability to dispose of a large amount of heat for a small amount of material loss. In general, the material may undergo sublimation or depolymerization (as is the case with most thermoplastic materials) or melting and vaporization (quartz is a good example of this). Examples of the process of heat disposal during ablation are shown in Fig. 13.(11)

A ceramic ablation shield is illustrated on the left of this figure. Aerodynamic heating of the virgin material causes it to flow as a liquid near the surface and part of this liquid layer is subsequently vaporized and is transported away by the airstream over the vehicle surface. The quartz ablation shield, presently

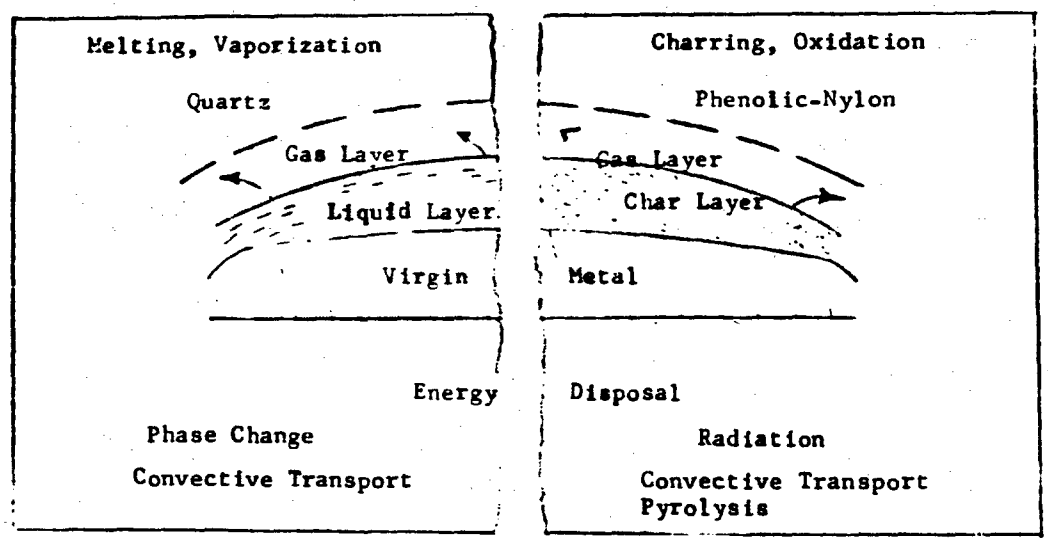

Figure 13 Ablative Concepts for Two Types of Materials (Ref.11)

used on the ICBM nose cone, behaves in this way. During ablation, heat is dissipated as latent heat in the phase change and is also transported away from the surface by convection in the liquid and gas layers.

(11)
On the right of Figure 13 is illustrated a charring ablation shield. In this case the shield may comprise a resinous material reinforced with glass or nylon. Pyrolysis of the virgin material produces a carbonaceous char which can sustain high surface temperatures. Heat energy is disposed by radiation from the surface, by convective transport, and by pyrolysis within the material.

The capability of the ablation material to dispose of heat cannot be defined without reference to the conditions of heating. The enthalpy of the airstream and the type of heating encountered (whether convective or radiative heating) may play an important part in the response of the material. Radiative heating becomes important when the air passing over the vehicle is sufficiently hot to radiate heat energy.

The interaction between a particular material and the gas boundary layer is, in general, a complicated process. The least interaction occurs for those materials which melt and flow without evaporation; consequently this class of materials is considered first. Though melting materials are probably the least interesting from a practical point of view, an understanding of melting is fundamental to an overall understanding of the ablation problem.

Very little coupling exists between the flowing liquid layer and the external gas boundary layer, especially if the liquid velocity is small compared with the external gas velocity and the melting temperature is much less than the

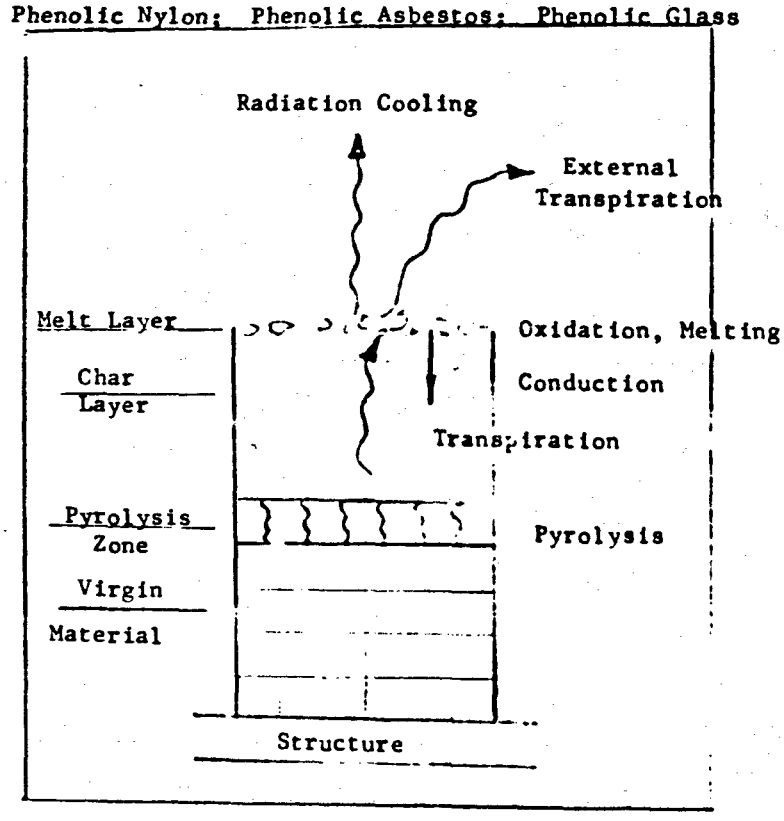

Figure 14 Composite Charring Ablation Phenomena (Ref.11)

gas stagnation temperature. The heat transfer, shear and pressure distribution can then be regarded as known and equal to their values for a solid boundary at the melting temperature.

Subliming ablation represents the other extreme from melting, and the absence of liquid flow simplifies the problem in some respects. Sublimation differs from melting in that now the interaction between the ablating material and the gas boundary layer is very important. The heat transfer is no longer independent of the ablation, as it was for melting; the injected vapor leads to a reduction in heating by the well-known transpiration or heat blocking effect.

In this category, most attention has been given the glass-plastic combinations and high viscosity glasses alone. The glassy materials have been found attractive because of their high viscosity, low thermal conductivity and rather high heat of evaporation. In addition, they exhibit good resistance to thermal stress. Plastics are combined with glass fibers or glass cloth for several purposes, such as to simplify fabrication and to reduce the thermal conductivity below that of the glass alone.

A typical composite ablation material consists of a phenolic or an epoxy resin reinforced with fiberglass or asbestos in the form of random or oriented fibers or in the form of a cloth.(11) The ablation shield used on the Mercury spacecraft, for example, was a combination phenolic-fiberglass material. Figure 14 illustrates the several phenomena that take place simultaneously during the ablation of such a material.(11) The material is shown in several layers; at the lower part of the figure is the virgin material which is attached

to the structure. Above the virgin material is a pyrolysis zone in which the phenolic resin starts to pyrolyze and form a char which accumulates to form a thick layer supported by the reinforcing material. The exposed surface of this reinforced char undergoes melting and oxidation and these two effects, together with aerodynamic shear and pressure forces, limit the growth of the char layer. Within the char, conduction of heat inwards to the pyrolysis zone is partly canceled by the transpiration of gases outward to the surface, and the subsequent introduction of these gases into the external flow provides further cooling. Since the char has a high carbon content, it sustains high surface temperatures and radiates an appreciable amount of heat. However, since pyrolysis takes place at a relatively low temperature, little conduction of heat takes place within the virgin material. This type of ablation has been investigated both experimentally and theoretically and appears to promise the solution to the heating problem encountered by manned entry vehicles.

The evaluation of charring materials is made particularly difficult by the fact that several effects take place simultaneously, and a thorough understanding of the effects of extreme heating requires both experimental and theoretical research on the ablation mechanism. (11)

IX. ABLATION MATERIALS -- Some generally desirable characteristics of ablation materials are as follows:

1. In general, gasification during ablation is desirable. The large amount of gas generated thickens the boundary layer and reduces the rate of heat transfer. Gasification products of low molecular weight enhance this effect because of their larger heat capacity and larger diffusion coefficients.

2. Ablation materials should have good thermal insulation characteristics

so that the ablation process, the loss of structural strength resulting from heating beyond the ablation zone, and the effect of local irregularities during ablation, are confined to the surface.

3. High heat of ablation -- The total amount of heat necessary to "wear-away" in this manner one pound of ablating material is referred to as the effective heat of ablation.

4. Low temperature of ablation

5. Ablation materials should have a high resistance to thermal and mechanical shock and be easy to fabricate in large sizes.

Materials of interest may be grouped as follows:

1. Plastics which depolymerize to a gas but do not liquefy (e.g., Teflon).

2. Materials which sublime and react with the constituents of dissociated air (e.g., graphite).

3. Materials which first melt and then vaporize (e.g., glass).

4. Composite materials, such as reinforced plastics which pyrolyze and char (e.g., phenolic-nylon).

The performance of an ablative material is a complex function of both materials and environmental variables, and since the design spectrum of hyperthermal environments is very large, it is impossible for a single material to be optimum for all types of environments. Each material exhibits optimum performance characteristics for a specific environment, and may even become unusable in other high temperature environments. It thus becomes necessary to develop a wide variety of ablators, which have the collective capability to accommodate the entire design spectrum of hyperthermal environments.

Many of these materials are shown in Fig. 15.[6] This list is not an all inclusive one, but it identifies materials which have exhibited relatively good performance in several different hyperthermal environments.

Fig. (16) gives the thermal properties for some typical ablative material.

Fig. (17) shows the role of ablation type cooling in the range of current reentry vehicle environments.[11]

X. Effects of Material Properties on Ablation Systems

During entry, the vehicle experiences a heating rate which increases (as the atmospheric density increaes) to a maximum value and then decreases as the vehicle is slowed down by atmospheric drag. This maximum value is plotted as the abscissa in Fig. 17 from 10 to 10^4 Btu/sq ft/sec.[11] The total heat flux experienced by the vehicle during the entry is plotted as the ordinate from 10^3 to 10^6 Btu/sq ft. The hatched line indicates the limits to which metallic heat shields can operate : a molybdenum shield can radiate about 40 Btu/sq ft/sec and a copper heat shield, such as that used on the early ballistic missiles, becomes so heavy that it is unfeasible for heat inputs greater than 10,000 Btu/sq ft. The broad arrow shows the thermal region in which the present and future entry vehicles will operate -- the upper half of the arrow corresponds to manned vehicles, the lower half, to unmanned vehicles which experience a shorter duration of heating. The direction of the arrow is that of increasing entry velocity.[11] It is clear from figure 17 that ablation materials play an extremely important role in the protection of vehicles returning from space.

MATERIAL PROPERTIES -- Heat of ablation. The extent to which the weight of a thermal protection system depends on the heat of ablation is shown on Fig. 18.[3] The weight of an ablating system is plotted as a function of the temperature of ablation.

HOMOGENEOUS ABLATORS

Plastics

- Polytetrafluoroethylene
- Polyethylene
- Polyamides
- Phenolics
- Modified Epoxies
- Expanded (Foamed) Resins
- Carbonized Resins

Ceramics

- Fused Silica
- Zirconia
- Magnesia
- Expanded (foamed) Ceramics

COMPOSITE ABLATORS

Reinforced Plastics

- Organic Resins Reinforced with Various Fibrous Materials such as Glass Fiber Reinforced Phenolic

Reinforced Ceramics

- Ceramic Filled Metal Honeycomb
- Metal Fiber Reinforced Ceramic

Impregnated Systems

- Organic Resin Filled Porous Ceramic
- Inorganic Particle Filled Refractory

Figure 15 Ablative Materials Composition (6)

As the temperature of ablation is increased from 200°F to 1,000°F, the weight of the thermal protection system increases. With a 12,000 Btu/lb heat of ablation, the weight increase is 2 pounds or 40 percent. With a lower heat of ablation, the weight increase is less.

As the temperature of ablation increases further, the weight approaches a constant value which is independent of the heat of ablation. The explanation for this is that, as the temperature of ablation increases, the system becomes more a radiative system and less an ablative system. Consequently, the properties of the material as an insulator and a radiator are more important than the heat of ablation.

Conductivity density product. The preceeding discussion has assumed a fixed value of the $k\rho$ product.(3) The effect of varying this product is shown in Fig. 19. The heating history is the same as before and a constant value of 8,000 Btu/lb is used for the heat of ablation. Values of $k\rho$ of 5, 15, and 30 are shown. This corresponds to the range of values for ablators and low density high temperature insulators. The weight of the thermal protection system is independent of the $k\rho$ product at a low temperature of ablation. As the temperature of ablation increases, the weight depends to a considerable extent on the $k\rho$ product. Here again, an increase in the temperature of ablation from 200° F to 1,000°F causes a considerable increase in weight. The increase in weight is greater with higher values of $k\rho$, and when $k\rho$ equals 30, the increase is almost 40 percent.

Note that, on both Figs. 18 and 19, the minimum weight thermal protection system is always obtained either with a low temperature ablating system or with a radiating system.

Material	Melting Point °R	Density Lb/Ft^3	Specific Heat BTU/Lb°R	Thermal Conductivity BTU/Ft-Sec-°R	Thermal Diffusivity Ft^2/Sec
Aluminum	1680	169	0.215	0.0366	0.00101
Beryllium	2800	114	0.52	0.0255	0.00043
Copper	2440	559	0.092	0.0632	0.00123
Graphite	6790	137	0.39	0.0051	0.000095
Iron	3260	492	0.11	0.0121	0.000224
Molybdenum	5220	637	0.061	0.0235	0.00060
Nickel	3110	556	0.105	0.0148	0.00025
Silver	2210	655	0.056	0.0672	0.00183
Tungsten	6630	1206	0.032	0.0323	0.00084

Figure 16 Thermal Properties of Ablative Materials

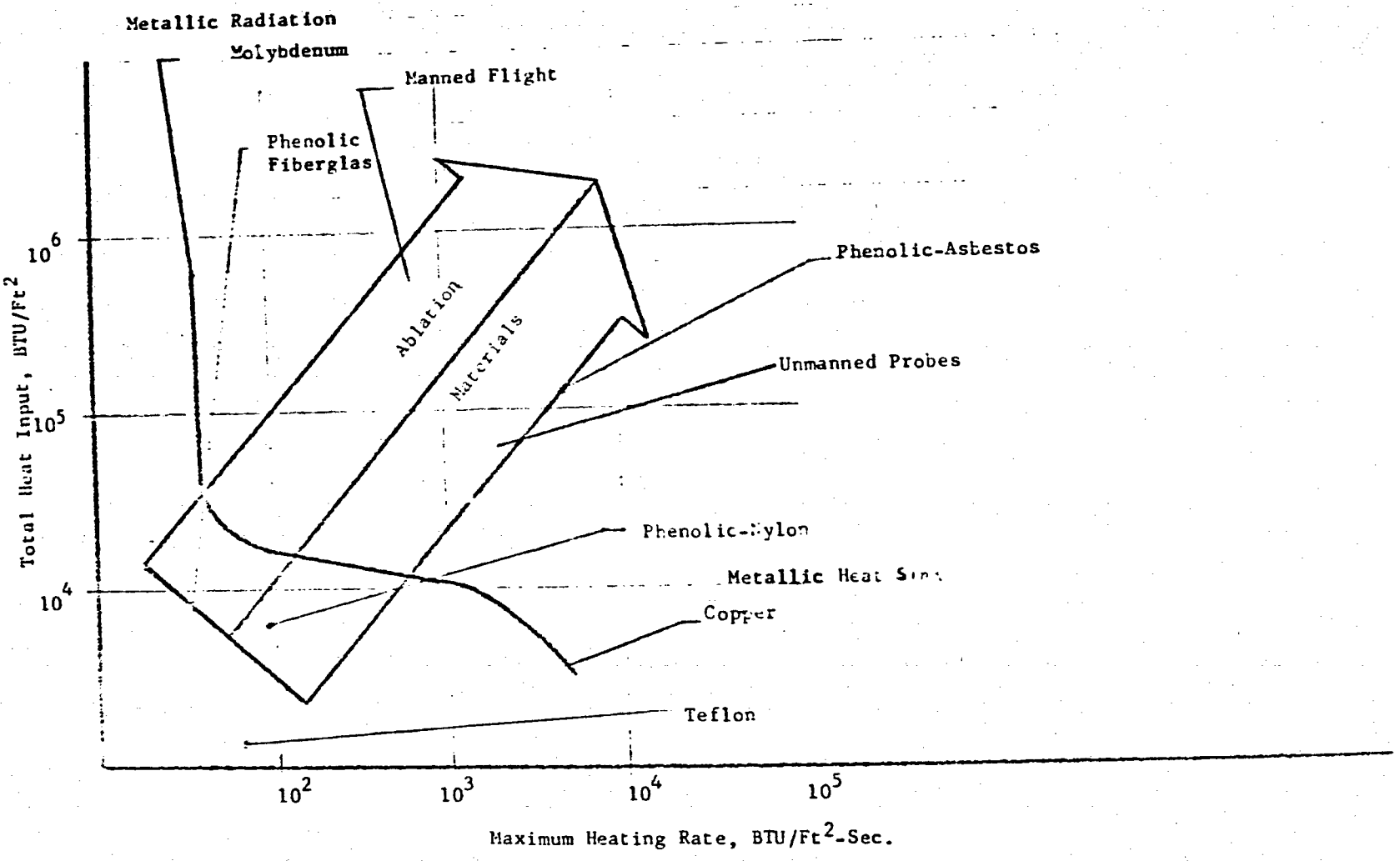

Figure 17 Entry Vehicle Heating Environment Showing Flight Tested Ablation Materials (Ref.11)

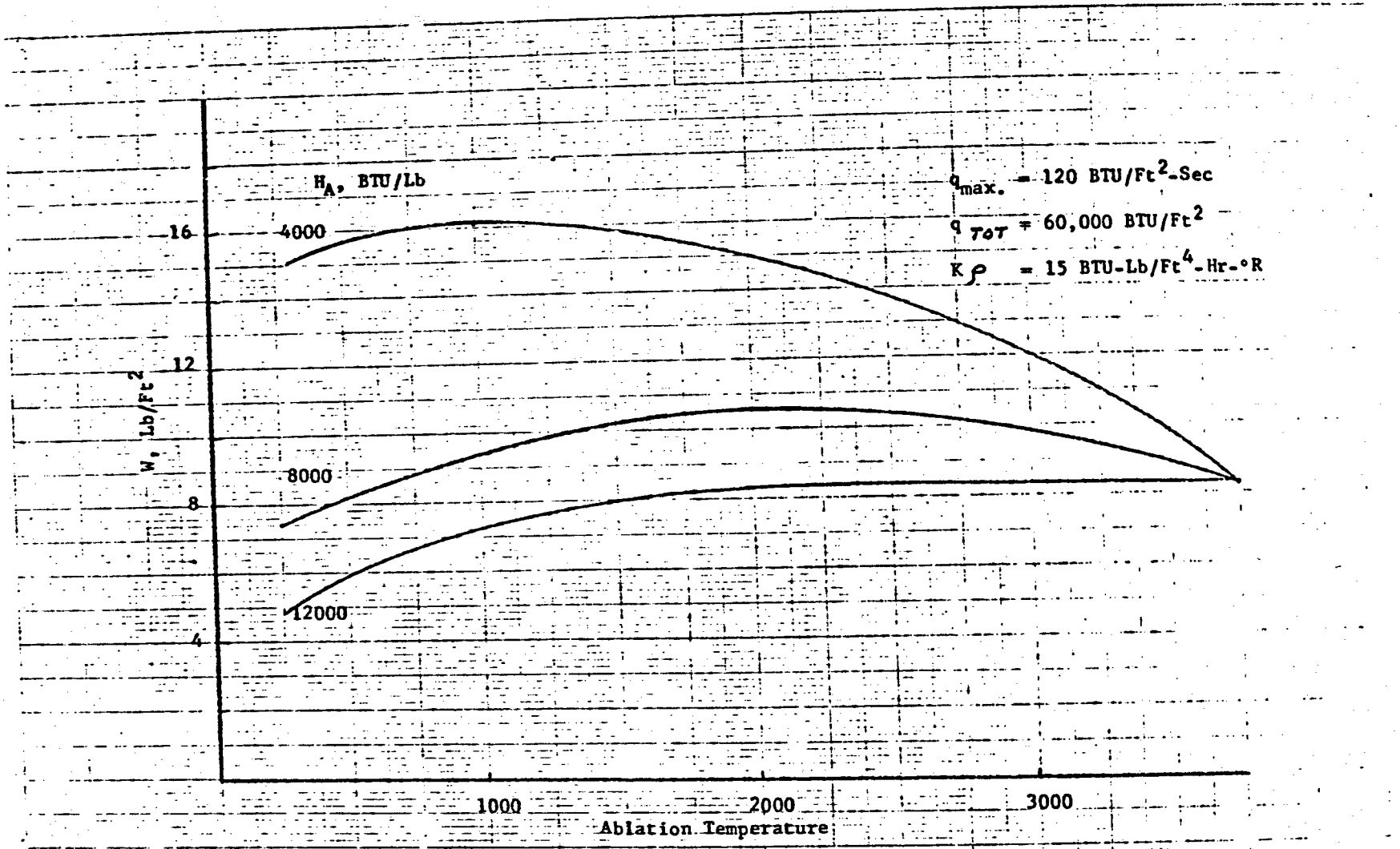

Figure 18 — Effect of Heat of Ablation on Thermal Protection System Weight (3)

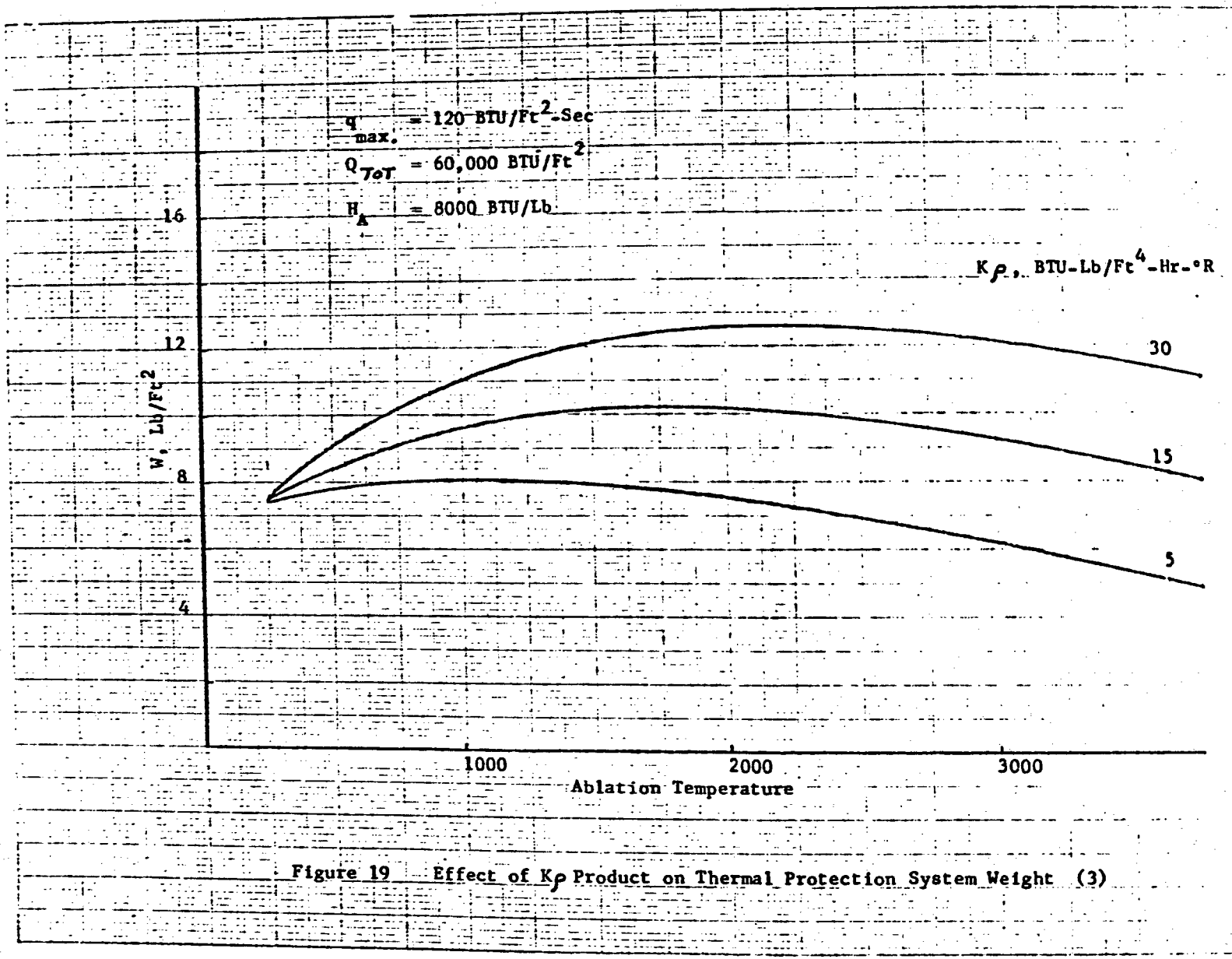

Figure 19 Effect of $K\rho$ Product on Thermal Protection System Weight (3)

In some cases the high temperature ablator had a better heat of ablation than the low temperature ablator and a better $k\rho$ product than the radiator. In general, it appears advisable to investigate the weight of the high temperature ablating system if either of these conditions exist.

XI Mass Transfer Cooling

Another method of cooling is mass transfer cooling which is essentially a simplified case of ablative cooling.[9] Mass transfer cooling, instead of generating a gas which is dependent on the boundary layer and material characteristics, independently introduces a foreign gas into the boundary layer. One method of accomplishing such cooling is to inject a gas of high specific heat directly into the boundary layer through openings in the surface, as shown in Fig. 20.[9] Here the temperature is controlled by forcing the coolant through a porous wall. From the vaporization process outward the actions resemble those involved in ablative cooling. As in the case of ablative cooling, the effectiveness of the injected gas as a boundary-layer shield is primarily dependent on the injected gas having a high specific heat and, secondly, on its having a small Schmidt number and a large Prandtl number. Hydrogen and helium are two gases that meet these requirements and perform well in this role.

XII Radiation Cooling Systems

In radiation cooling an outer layer of high-melting point material is provided. The purpose of this layer is to reject a large quantity of heat by radiation, thus maintaining the substructure at a low enough temperature to withstand the required loading.

Figure 21 shows three types of radiative-protected structure.[12] Since the heat radiated from the shield is proportional to the fourth power of the temperature, the higher the operating temperature, the more efficient the shield. Likewise,

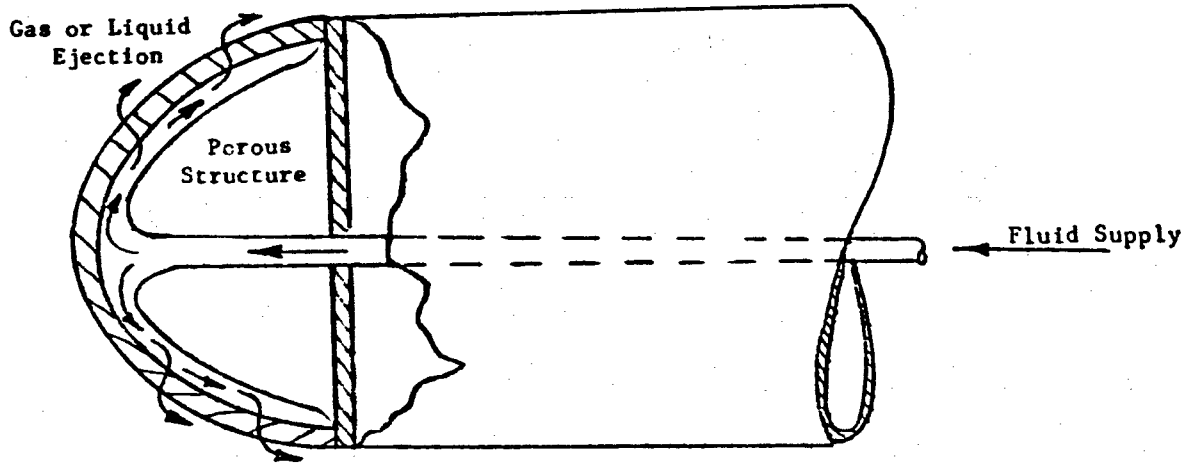

Figure 20 Mass Transfer Cooling (Ref. 9)

a high value of emissivity (ϵ) at the operating temperature is important. While this operating temperature must be consistent with the shielding material and the insulation if used, the operating temperature will have to be in excess of 1800° F for the quantity of heat rejected by this system to be of importance.

This method of heat protection is not useful where the boundary-layer temperature is extremely high, as in the case of a non-lifting reentry.(12) On the other hand, when moderately high fluxes are experienced for relatively extended periods of time, it does offer advantages.

For a glide-reentry type of vehicle, this kind of heat protection would be most useful. In the uninhabited portion of such a lifting vehicle the radiation principle, such as shown in Fig. 21,(9) could be used to advantage. The structure shown might be a section of an aerodynamic surface used to provide lift. For this surface a pronounced difference will exist between the windward and leeward sides, the former being at the highest temperature. By radiating and conducting some heat from the hotter surface to the cooler surface, the efficiency of the radiative capacity of the leeward surface is improved.

The success of the radiative system depends on the introduction of an effective heat barrier between the boundary layer and structure, such that most of the heat will be re-radiated into the atmosphere. Such a heat barrier must meet three distinct and unrelated requirements.(12) It must have a low $k\rho$ (conductivity x density) value; it must have adequate structural strength to function as the exterior surface of the vehicle, and, it must have sufficient temperature capability to maintain temperature levels that are necessary for the re-radiation of heat into the atmosphere.

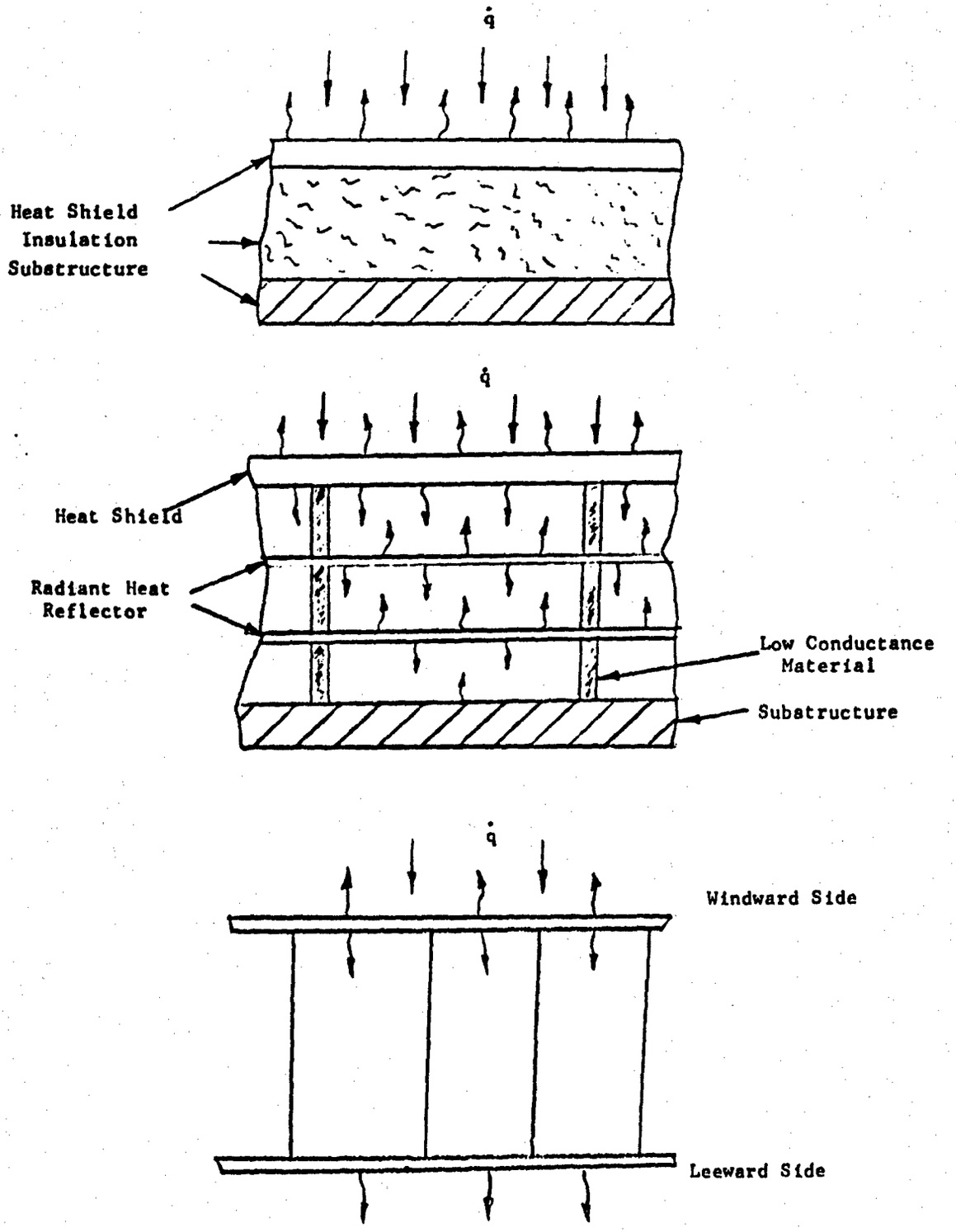

Figure 21 Radiant Types of Heat Shields (Ref. 9)

Some organic materials meet all these requirements quite well, but only up to 800°F. Above this temperature, no currently available material meets the previously stated three requirements adequately and simultaneously. Materials with excellent insulation characteristics, such as fibers, ceramics and powders, have far too inferior mechanical strength. On the other hand, metals, with superior mechanical properties, have k values that may be 20,000 times that of the k of the best attainable insulators.

The radiative systems fall in two distinct classes having considerably different thermal efficiences.(12) The more efficient type consists of a metallic outer shield backed with a low density fibrous insulation. This configuration is limited by the maximum temperature which the metal shield can withstand. The development of refactory metal shields capable of operating at a temperature of 3,000°F or nonmetallic shields capable of operating at temperatures up to 4,000°F would greatly increase the region for application of this concept.

When the radiation equilibrium temperature is greater than 2,500°F, but less than about 4,000°F, the porous ceramics offer a possible solution. However, porosities of 80 to 90 percent will be required in order to achieve reasonable weight.

XIII. Selection of Appropriate Protection System

Now, using the concepts which have been discussed and making assumptions as to the values of material properties, it is possible to indicate the type of thermal protection system which will be appropriate to the various areas of the vehicle band.(3) This information is shown in Fig. 22. For heating rates

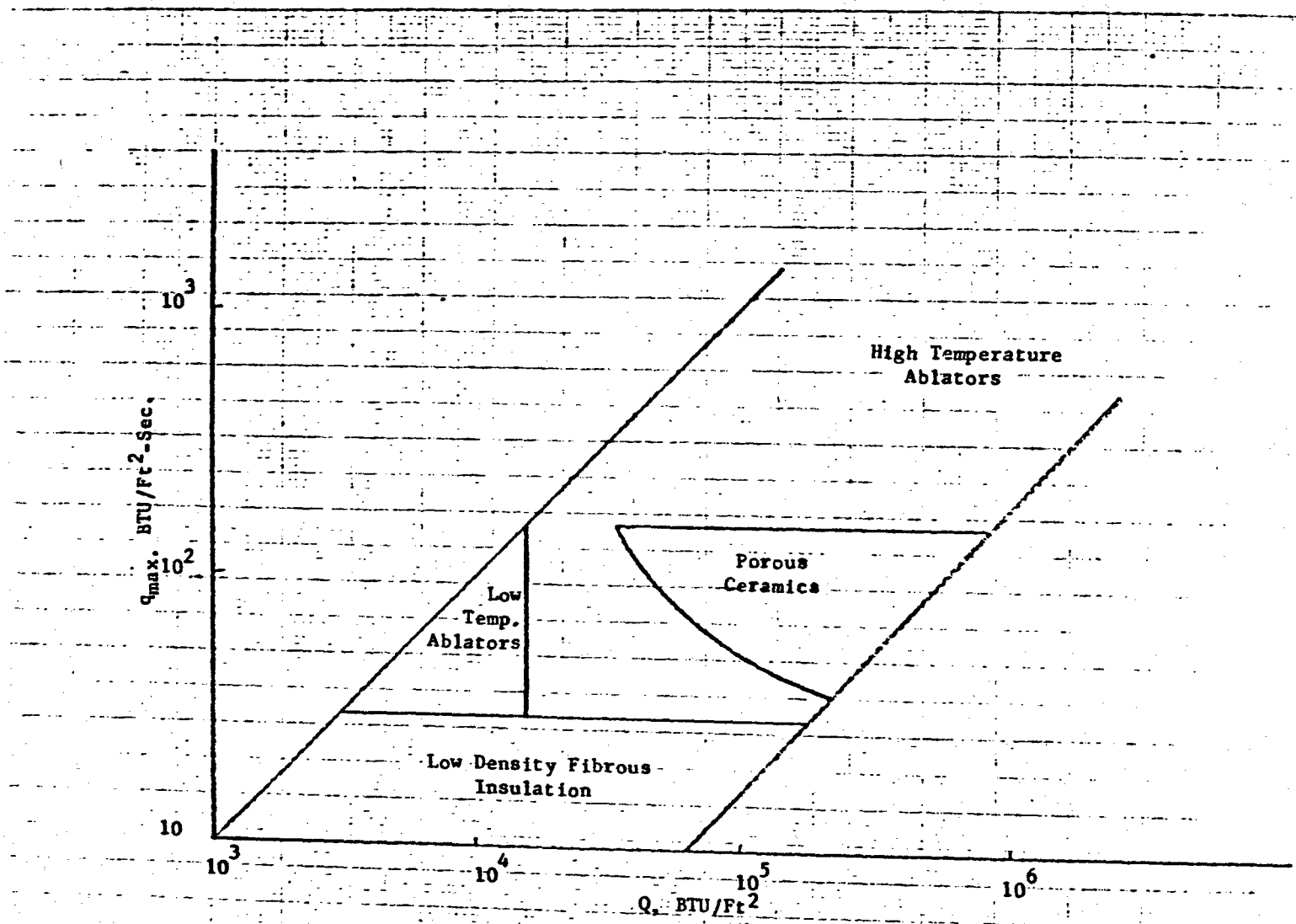

Figure 22 Probable Design Chart (3)

producing maximum equilibrium temperatures below 2,500°F, the use of low density fibrous insulations with metallic outer shields is clearly indicated. Weights less than 3 lb/ft^2 should be attainable even at the higher heat loads.

With maximum equilibrium temperatures between 2,500°F and 4,000° F, low temperature ablators, high temperature ablators, and porous ceramics may find application. At the lower heat loads, low temperature ablators will generally give minimum weight. At moderate heat loads, weights of all three systems may be close together and the choice for design will depend on available material properties. At higher heat loads, optimum design will probably use porous ceramics, but a low density high temperature ablator could probably be used with little weight penalty in part of this region.

For areas having a maximum equilibrium temperature greater than about 4,000° F, it will be necessary to use an ablating thermal protection system. There may be a small area for use of low temperature ablators at the lower heat loads. At higher heat loads, high temperature ablators will provide minimum weight.

XIV. System Weight and Design Concepts

An estimate of the thermal protection system weights which will be required for the different regions of the manned reentry band is given on Fig. 23.(3) The exact weights required will depend on available materials. Near the low L/D edge of the band with maximum heating rates below about 300 Btu/ft^2-sec, system weights of 3 to 8 lb/ft^2 are encountered. Considerable experience has already been accumulated in the design of shields of these weights for ballistic vehicles. Experience in other areas is limited.

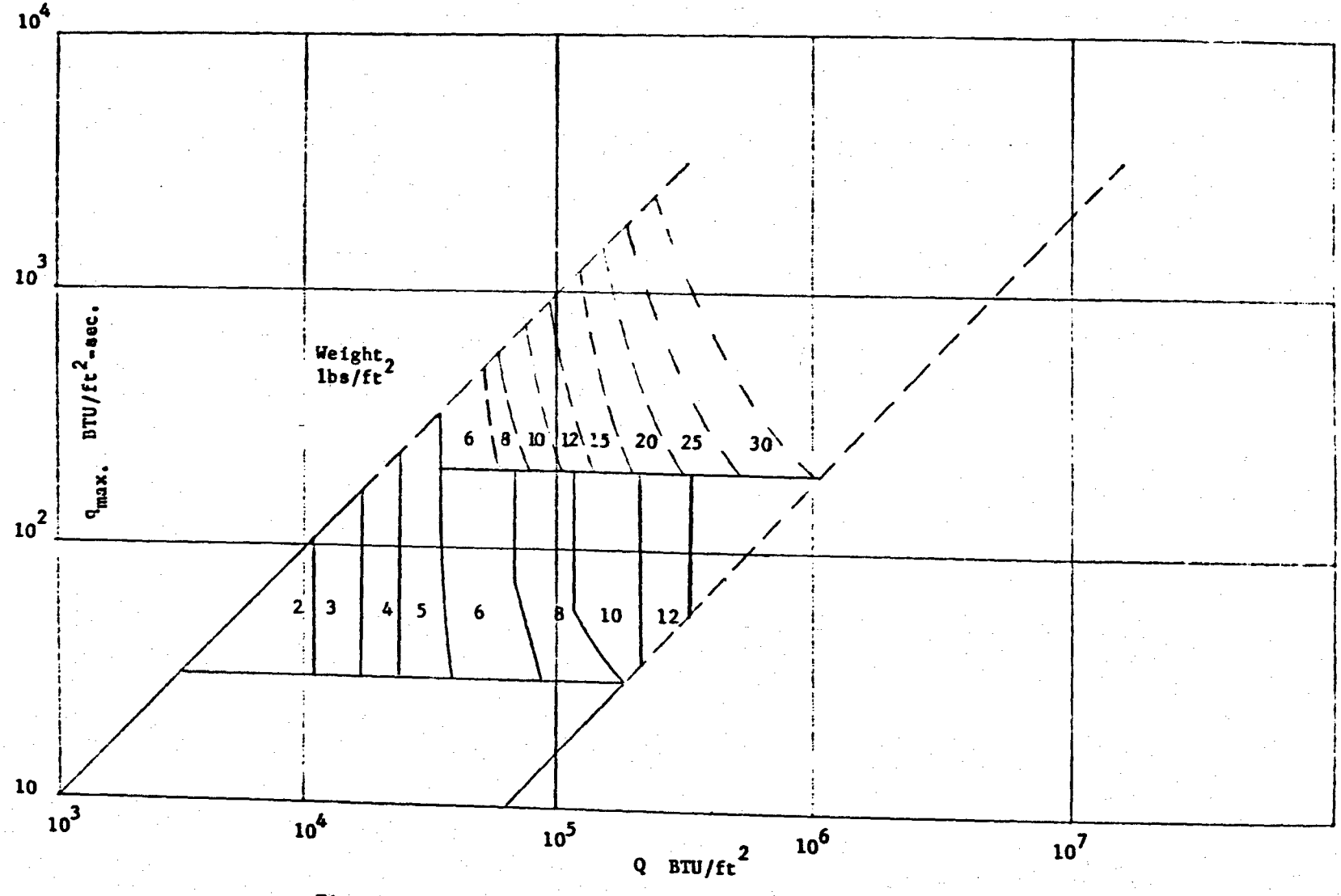

Figure 23 Total Weight Estimates of Thermal Protection Systems (3)

It may be helpful (3) to summarize the important parameters for each of the thermal protection systems. This information can then be used to estimate the effect of changing properties on weight and region for design. The heat of ablation is the most important property of a low temperature ablator. The $k\rho$ product is the most important property of a radiative system, or a heat sink system (assuming, of course, that a high surface emissivity is attained). There are three cases in which a high temperature ablator may provide minimum weight design as follows:

1. The high temperature ablator has a higher heat of ablation than a low temperature ablator, and a moderately low value of the $k\rho$ product.
2. The high temperature ablator has a lower $k\rho$ product than the available radiators, and a moderately high heat of ablation.
3. The maximum equilibrium temperature is too high for the use of radiators so that an ablative system must be used. The choice between a high temperature ablator and a low temperature ablator will depend primarily on the $k\rho$ product of the available high temperature ablators.

Weight and design concepts are also influenced by the heating conditions encountered. The weight of a low temperature ablating system increases directly as the heat load, while the weight of a radiating system increases as the square root of the total heat load. Therefore at higher total heat loads, the radiative system appears more attractive.

An efficient thermal protection system must dispose of most of the incident heat at the outer surface. The remainder may be absorbed by a heat sink or coolant at the inner surface. Heat may be either radiated or absorbed by ablation at the outer surface, and both mechanisms may be employed simultaneously. Some systems that have been analyzed previously are shown in

Fig. 24.[12] These systems are all characterized by an insulating layer that remains homogeneous through its entire depth throughout the heating period and will be defined as simple systems to distinguish them from composite systems. The ablative system consists of a layer of ablating material, part of which is not ablated and serves as insulation and a low level cooling system.

The radiative systems, shown in Fig. 24, fall in two distinct classes having considerably different thermal efficiencies. The more efficient type consists of a metallic outer shield backed with a low density fibrous insulation. This configuration is limited by the maximum temperature that the metal shield can withstand. The porous ceramic shields are less efficient but are capable of operating as temperatures up to 4000°F. With radiation equilibrium temperatures greater than the maximum ceramic temperature, the ceramic may function as an ablating material.

The composite shields are shown also in Fig. 24. The series-type shield consists of a high temperature ceramic insulator at the outer surface and an efficient fibrous insulator at the inner surface. This shield is a combination of two radiative shields shown in the upper portion of Fig. 24. The impregnated shields consist of an insulating shield impregnated with low temperature pyrolyzing substance. The insulating shield may be either a porous ceramic or a char layer that is formed during heating.

XV. System efficiencies

The concept of thermal protection system efficiency can be used to compare the relative merits of various systems. System efficiency is defined as the total heat load divided by the required system weight.

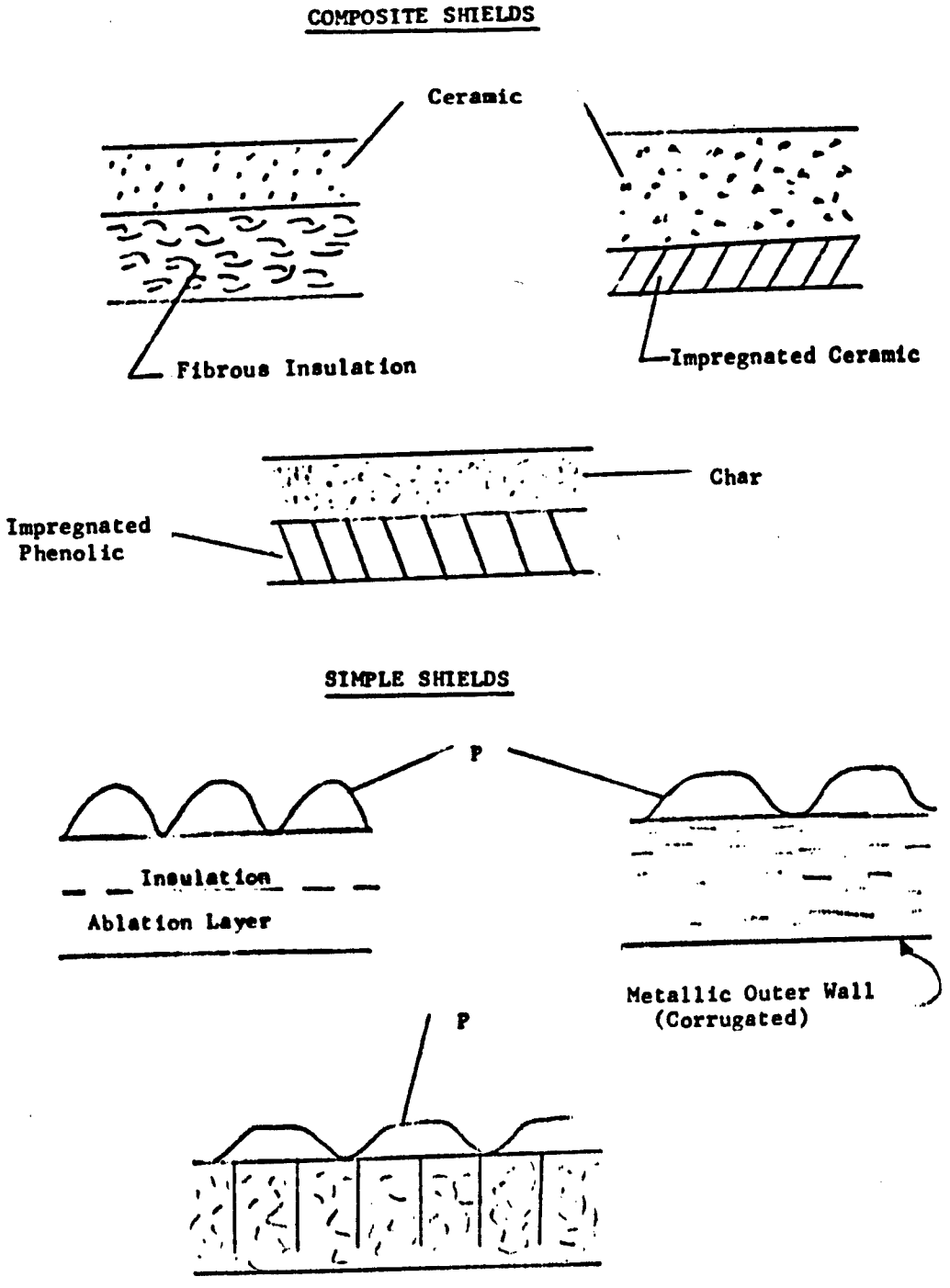

P = Structural Panel with Water Cooling (T = 200°F)

Figure 24 Thermal Shields (Ref. 12)

The efficiencies of the simple systems are plotted in Fig. 25 (12) as a function of total heat load. The efficiency of an ideal low temperature ablating system (that is, one for which no cooling is required) is independent of the total heat input and is equal to the heat of ablation. Average heats of ablation depend on the average enthalpy difference across the boundary layer during entry. Representative values of the average heat of ablation for available low temperature ablators are 4000 Btu/lb for entry at satellite velocity and 6500 Btu/lb for entry at escape velocity. However, available low temperature ablators do not ablate at the desired back surface temperature, and considerable additional weight may be required for back surface temperature control. Therefore, the efficiencies shown in Fig. 25 represent the maximum possible efficiencies for low temperature ablators, and it can be seen that low temperature ablators have application only at low heat inputs.

For low density fibrous insulation with a metal exterior shield and for porous ceramic shields, the efficiency increases as the total heat input increases. It is to be noted that both systems have a limiting value of heat flux which corresponds to the maximum temperature that the exterior surfaces can withstand. (Assume T max = 2500°F for metallic skin and T max = 4000°F for ceramic.) The efficiency of the ceramic shield is less than half that of the system employing a metallic shield. Consequently, when it becomes necessary to change from metallic construction to ceramic construction (because of equilibrium temperatures too high for metals), a step increase in weight occurs.

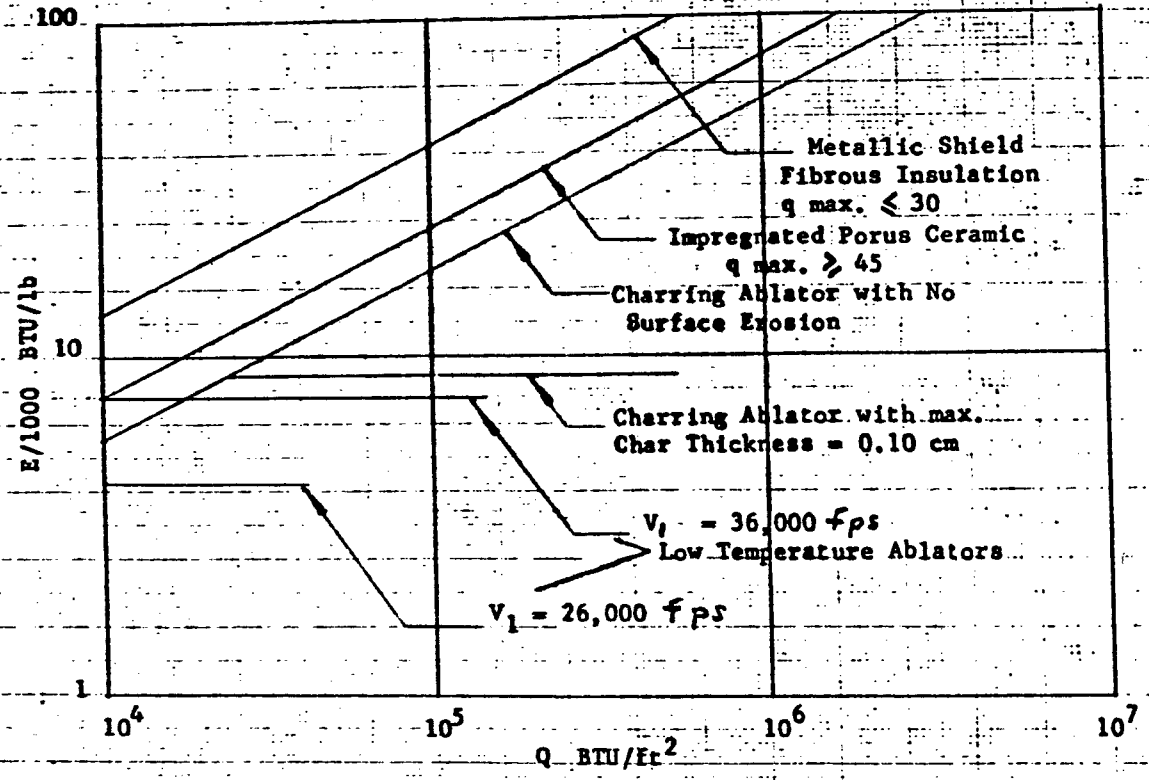

Figure 25 Efficiencies of Thermal Protection Systems (12)

By using composite shields, the efficiency level for the ceramics can be increased, and the step increase in weight at 30 Btu/ft^2-sec can be eliminated. The efficiencies of composite shields are also indicated in Fig. 25. For heating rates up to 30, the fibrous insulation with metallic shield still provides highest efficiency. For heating rates between 30 and 45 Btu/ft^2-sec, highest efficiency is provided by the series-type composite shield. The range of application of these systems using fibrous insulation is limited by the temperature resistance of the fibers. The range might be greatly extended by the development of systems employing high temperature fibers and graphite shields.

XVI Aeronca Composite Thermal Shield

A composite thermal protection system (Thermantic Structure) has been developed by Aeronca Manufacturing Corporation and is shown in Fig. 26.[13] Aeronca has in recent years been engaged in the development of materials and structures to withstand temperatures in excess of 3000°F for extended periods of time (approximately one hour) and to resist the severe noise and dynamic loads associated with space vehicle flight. Aeronca's basic approach to the composite heat shield concept has been to utilize a reinforced ceramic heat shield to protect the vehicle from its heating environment. The heat shield, made of a low density ceramic foam reinforced with a honeycomb cell structure, is capable of maintaining an internal temperature suitable for the survival of both man and sensitive equipment. The thermantic structure uses a conventional load bearing panel fabricated from alloy sheets brazed to stainless steel honeycomb and this panel brazed to the ceramic honeycomb reinforcement. This "Astroshield" concept offers the combined advantages of high temperature resistance, lightweight, thermal shock resistance, chemical stability and high strength. In the course of this development program, several lightweight

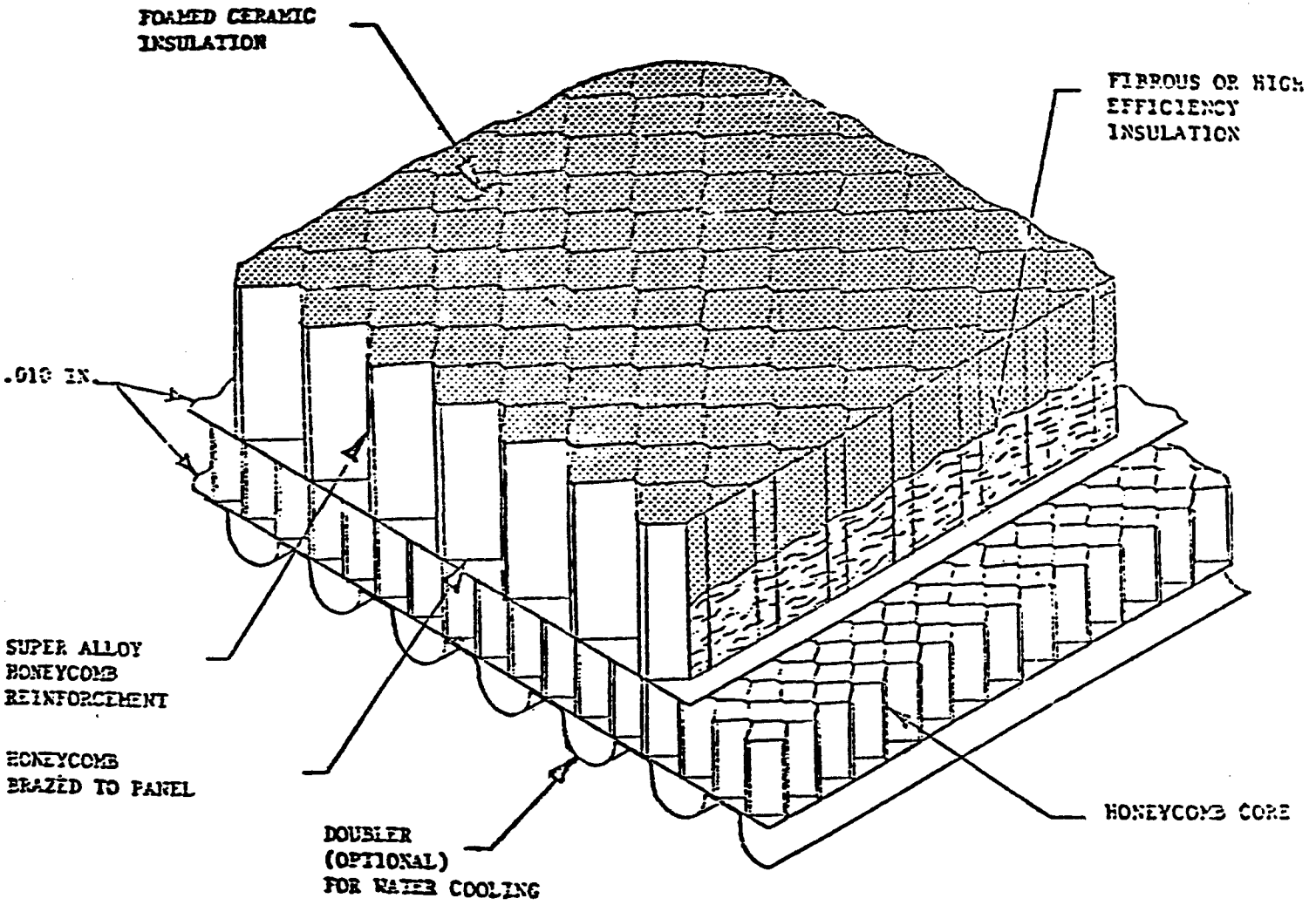

AERONCA THERMANTIC CONSTRUCTION

FIGURE 26

ceramic compositions have been fabricated in porous forms with satisfactory mechanical and thermal properties for re-entry vehicle structures. The most promising have been silica (S.G. .5 and 3000° F M.P.), alumina (S.G. .5 and 3400°F M.P.) and zirconia (S.G. 1.1 and 4200°F. M.P.). These ceramics when reinforced with superalloy or refractory metal honeycombs form durable insulating heat shields which radiate almost all heat input back into space. High emissivity ceramic coatings reduce radiant heat transmission through the structure to approximately 2% during re-entry flight.

The Aeronca Thermantic "Astroshield" concept is oriented towards several applications involving space vehicles. The radiation cooled structure can be used for almost the entire external surface of lifting body shaped vehicles, nose caps, leading edges, portions of fuselages and winged sections of aerospace vehicles.

One such application of Aeronca's composite heat shield concept has been in the fabrication of a section of the forebody of the re-entry vehicle shown in Fig. 27. The green section of the vehicle is that being fabricated by Aeronca. Fig. 28 shows the trajectory characteristic of this type of vehicle. Notice that the vehicle re-enters the atmosphere with a superorbital velocity of 36,000 FPS. Also shown on this figure are the different regions of hypersonic flow explained in Fig. 1 and the region in which maximum radiative and convective heating occurs. It should be pointed out here that the radiation heating is a characteristic environment of the region around the nose cone (stagnation point). Figure 29 shows the stagnation point and forebody heat fluxes and radiation equilibrium temperatures as a function of time. Fig. 30 shows the typical response of a Thermantic panel to a surface temperature environment

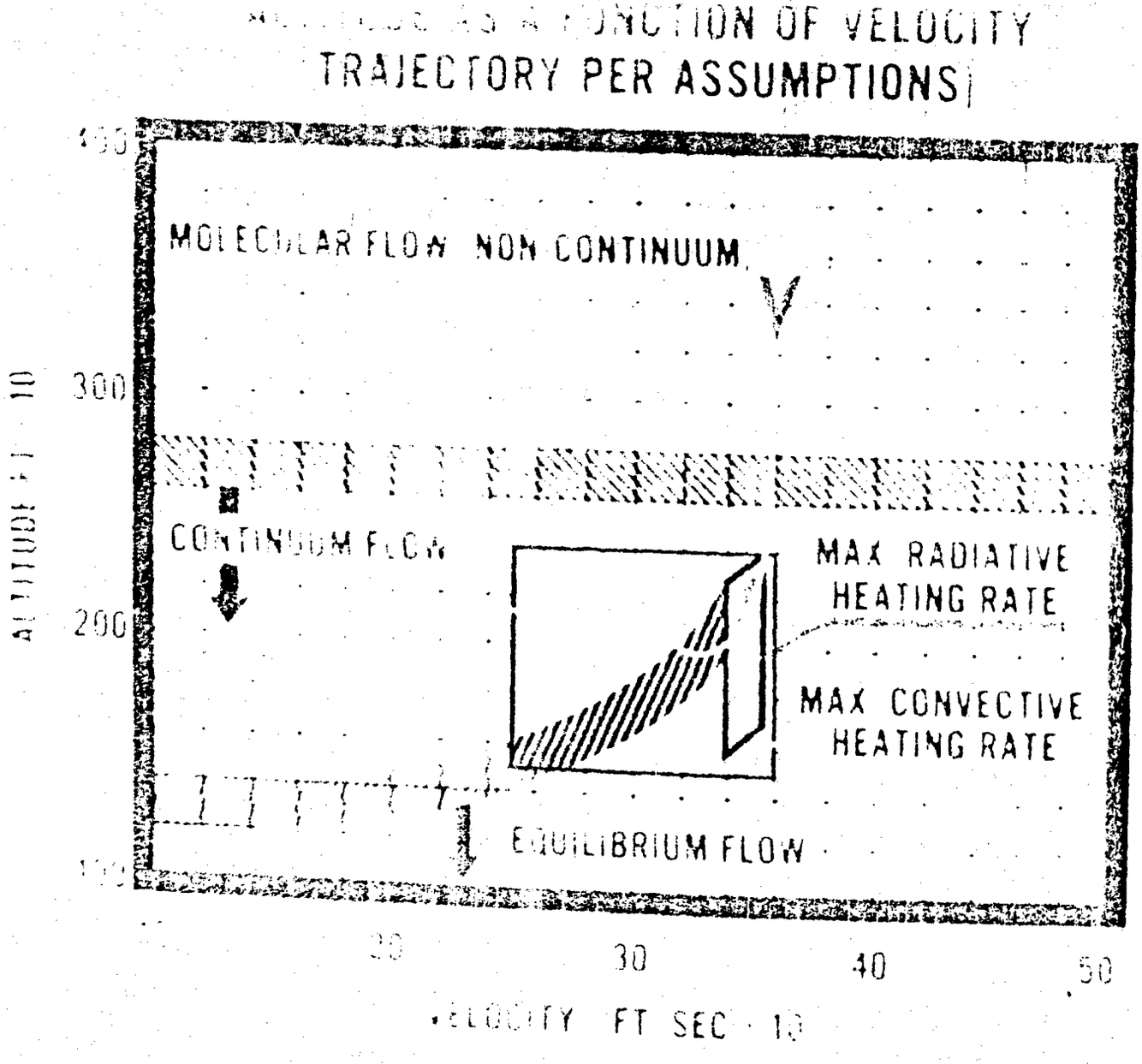
FUNCTION OF VELOCITY
TRAJECTORY PER ASSUMPTIONS
MOLECULAR FLOW NON CONTINUUM
CONTINUUM FLOW
MAX RADIATIVE HEATING RATE
MAX CONVECTIVE HEATING RATE
EQUILIBRIUM FLOW
300
200
30
40
50
FT SEC

FIGURE 27

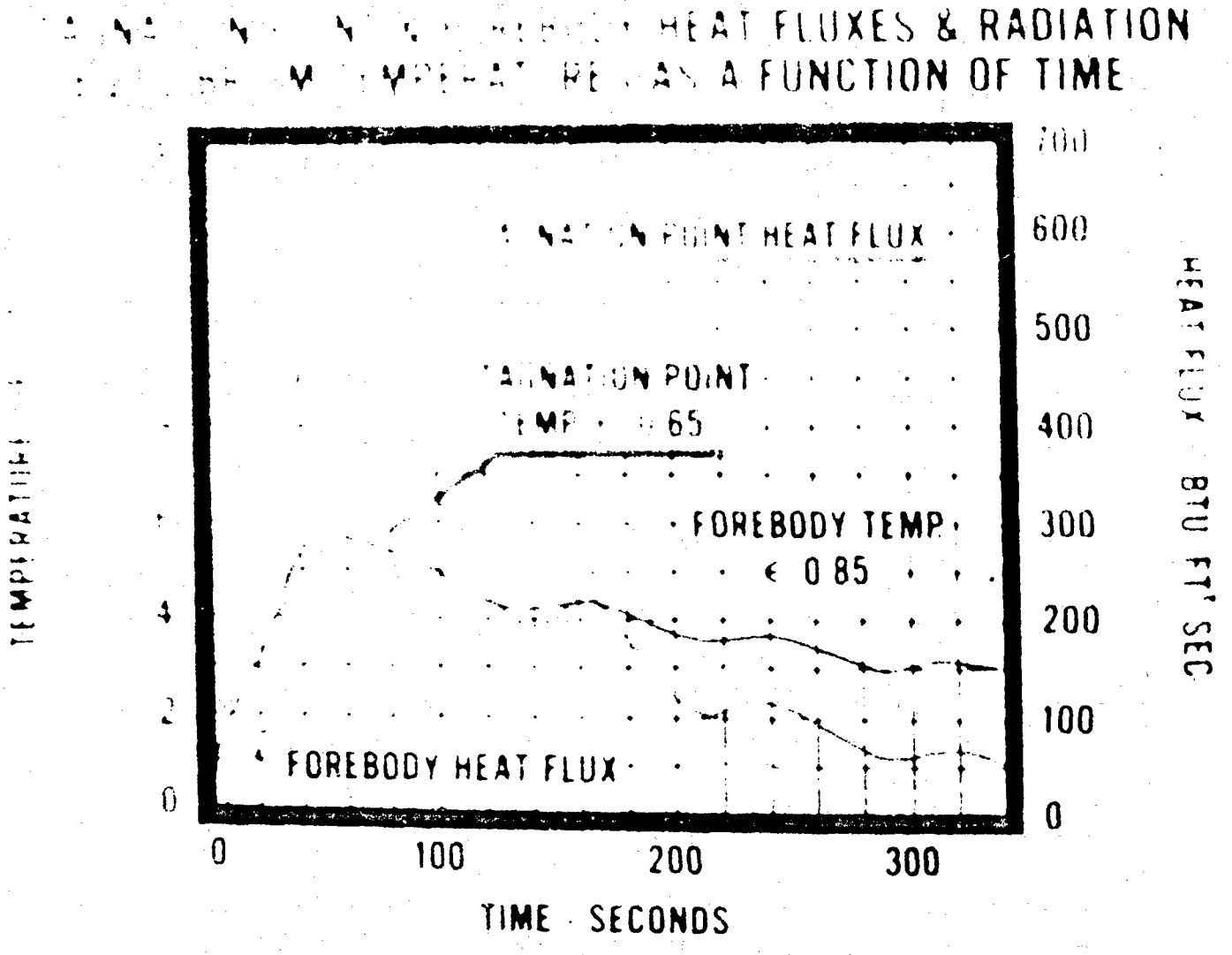
HEAT FLUXES & RADIATION
A FUNCTION OF TIME
HEAT FLUX
600
500
400
300
200
100
0
FOREBODY TEMP
ε 0 85
FOREBODY HEAT FLUX
0
100
200
300
TIME SECONDS

Figure 28

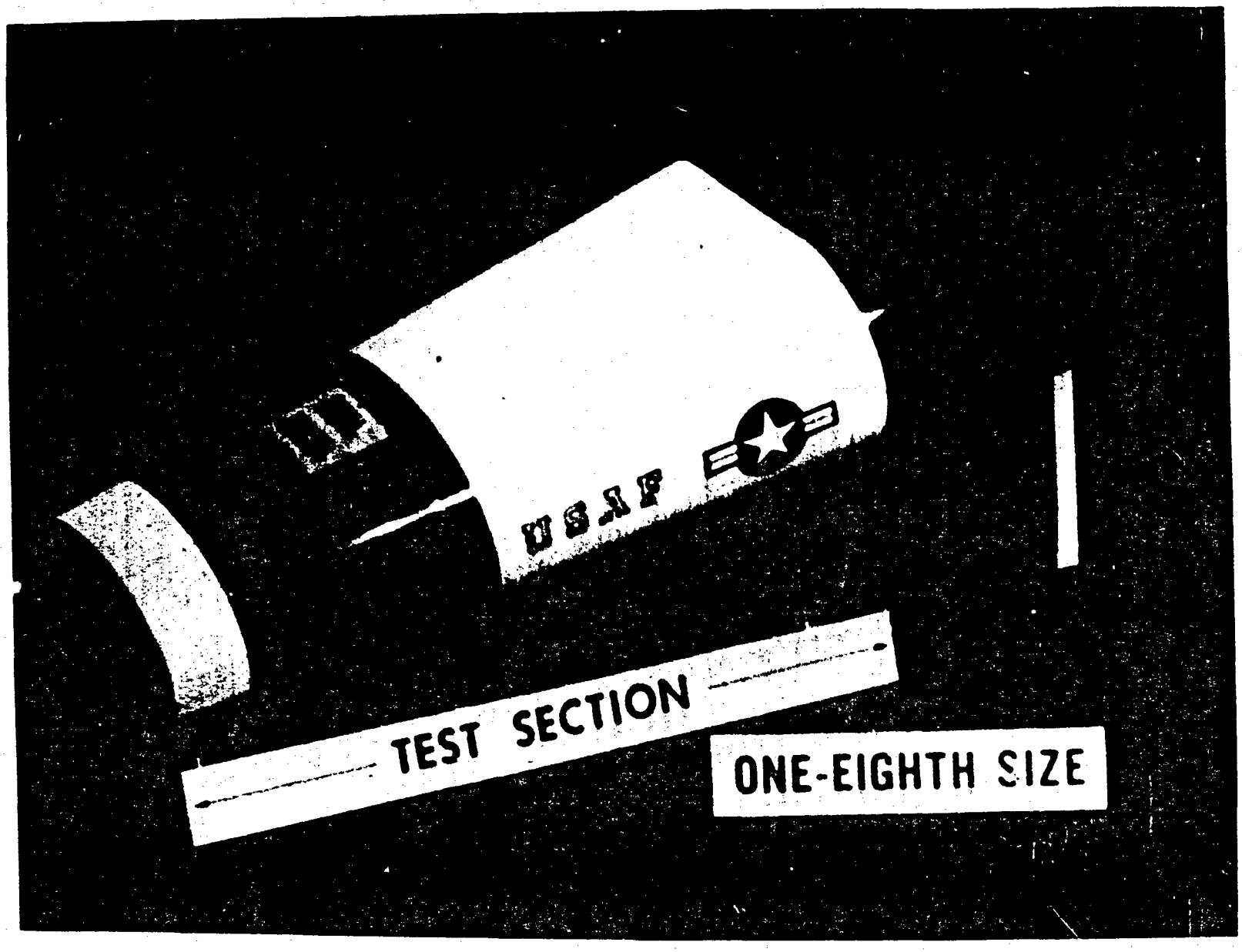

FIGURE 29

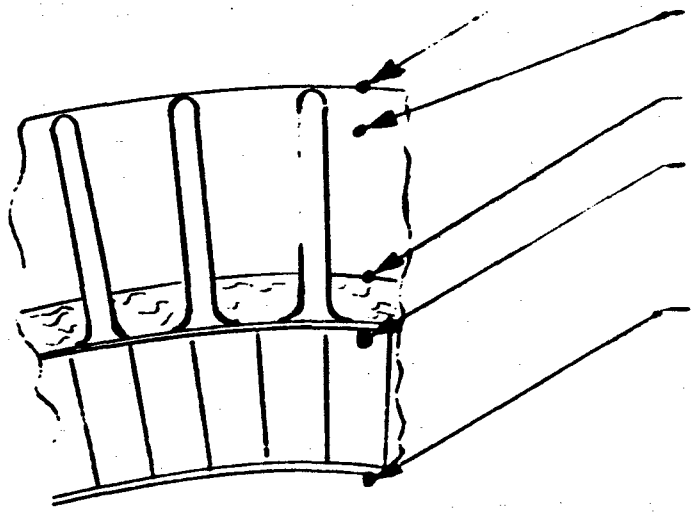

SURFACE EMISSIVITY	0.6	0.9
OUTSIDE SURFACE TEMP., °F	4300	3840
TEMP. OF CERAMIC 1/4" BELOW SURFACE, °F	3530	3160
TEMP. AT INTERFACE OF CERAMIC AND FIBROUS INS., °F	2170	1920
TEMP. AT HONEYCOMB FACE, °F	1295	1190
BACK SURFACE TEMP., °F	800	750
NET HEAT TRANSFER BTU/sec-ft^2	0.57	0.50
OVERALL CONDUCTANCE BTU/Hr-ft^2-°F	0.588	0.588

Figure 30

CURVED PANEL THERMAL DATA
FOR EXPOSURE AT 150 BTU/sq. ft.-sec.

of 4300°F. Figs. 31 and 32 show sections of the fabricated forebody of the reentry vehicle shown in Fig. 27. These views clearly show the various components of the Aeronca "Astroshield" composite structure.

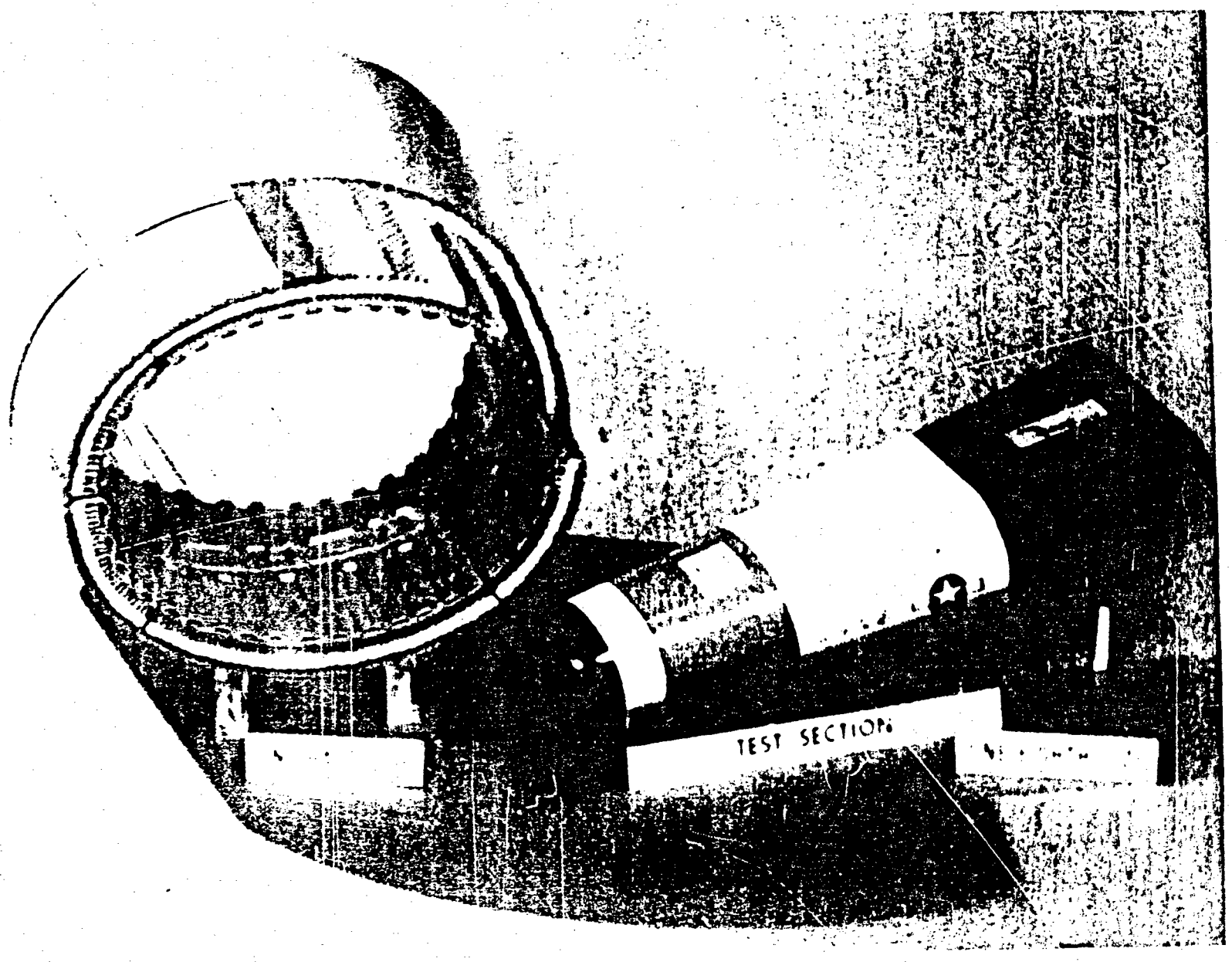

FIGURE 31

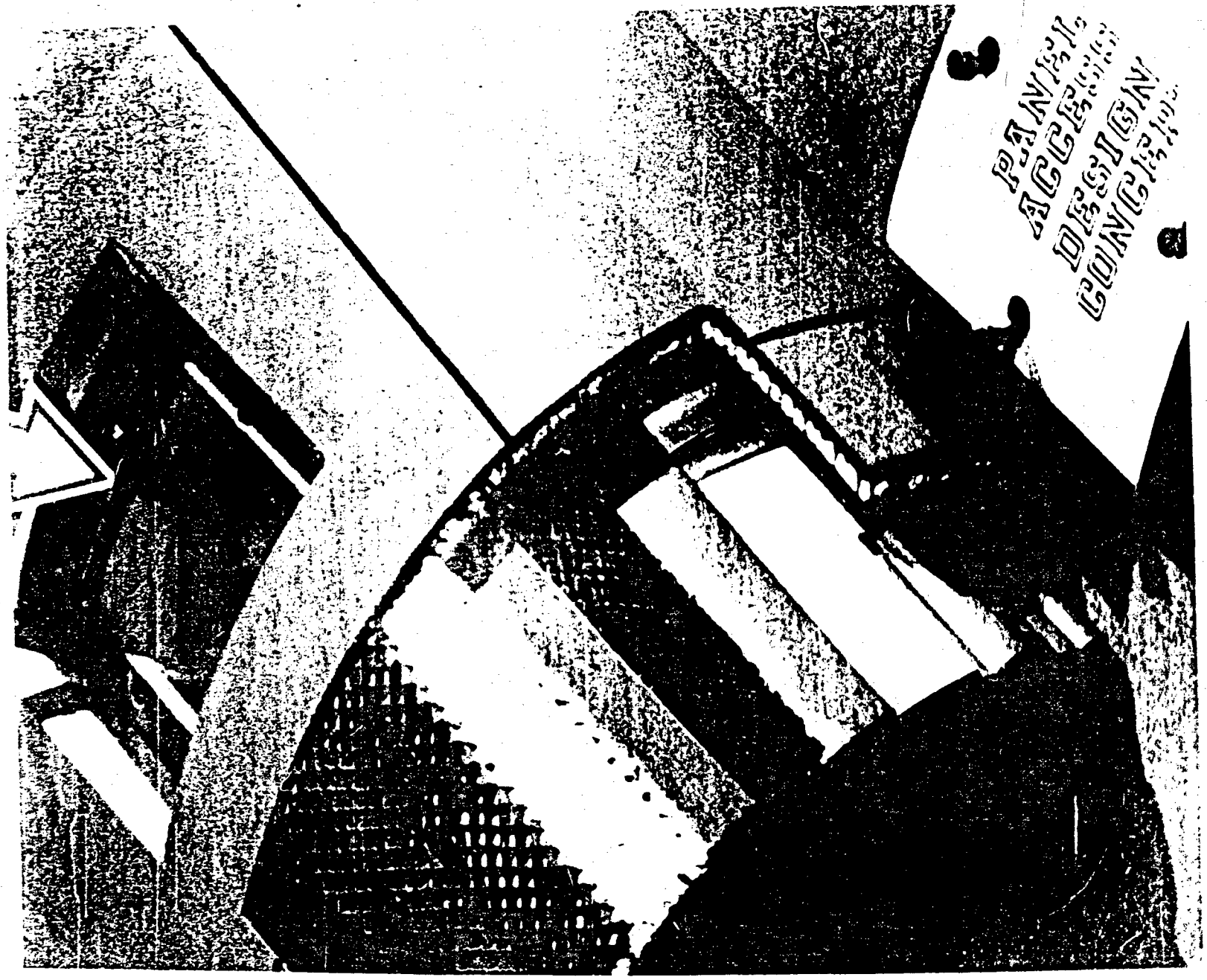

FIGURE 32

References

1. S. M. Scala, AFIAS "The Hypersonic Environment", Aerospace Engineering Jan., 1963.
2. W. R. Niehaus, "Hypersonic Ballistic Range", Presentation at Ames Research Center, NASA, May, 1958.
3. R. T. Swann, "An Engineering Analysis of the Weights of Ablating Systems for Manned Re-entry Vehicle", Ballistic Missile and Space Technology, Legally, D.P., Academic Press, 1960.
4. E. E. Mathauser, "Research, Design Considerations and Technological Problems of Structures for Winged Aerospace Vehicle", NASA SP-11, Vol. II, Nov., 1962.
5. I. E. Garrick, FIAS, "A Survey of Aerothermoelasticity", Aerospace Engineering, Jan., 1963.
6. J. M. Kelble, J. E. Bernadoa, "High Temperature Nonmetallic Materials", Aerospace Engineering, Jan., 1963.
7. W. R. Laidlaw, AFIAS, J. H. Wykes, AFIAS, "Potential Aerothermoelastic Problems Associated with Advanced Vehicle Design", Aerospace Engineering, Jan., 1963.
8. ASD TR7-845 (I).
9. L. H. Abraham, "Structural Design of Missiles and Spacecraft", McGraw-Hill, 1962.
10. E. P. Bartlett, "Thermal Protection of Rocket-Motor Structures", Aerospace Engineering, Jan., 1963.
11. L. Roberts, "Ablation Materials for Atmospheric Entry", NASA SP-11, Vol. II, Nov., 1962.
12. R. T. Swann, "Composite Thermal Protection Systems for Manned Re-entry Vehicles", ARS Journal, Feb., 1962.
13. ASD TR7-845 (I-IV).